INTERNATIONAL JOURNAL FOR NUMERICAL METHODS IN ENGINEERING
Int. J. Numer. Meth. Engng 2001; **50**:1469–1499

Finite element approximation of piezoelectric plates

F. Auricchio[1], P. Bisegna[2] and C. Lovadina[3,*,†]

[1]*Department of Structural Mechanics, University of Pavia, 27100 Pavia, Italy*
[2]*Department of Civil Engineering, University of Roma 'Tor Vergata', 00133 Rome, Italy*
[3]*Department of Mechanical and Structural Engineering, University of Trento, 38050 Trento, Italy*

SUMMARY

A Reissner–Mindlin-type modellization of piezoelectric plates is here considered in a suitable variational framework. Both the membranal and the bending behaviour are studied as the thickness of the structure tends to zero. A finite element scheme able to approximate the solution is then proposed and theoretically analysed. Some numerical results showing the performances of the scheme under consideration are discussed.

KEY WORDS: piezoelectricity; plates; mixed finite elements

1. INTRODUCTION

In recent years, a growing interest towards the study of piezoelectric bodies has been devoted by the engineering practice. The main reason consists in the fact that piezoelectric materials are widely used as sensors and actuators in structure control problems.

In the present paper, we consider a piezoelectric plate, comprised of homogeneous linearly piezoelectric transversely isotropic material (Hermann–Maugin class ∞mm [1]), with the axis of transverse isotropy oriented in the thickness direction. Many different modelizations of this body are available in the literature (cf. References [2–9], for instance). Among them, the one proposed in Reference [10], based on Reissner–Mindlin kinematical assumptions, is considered in this work. We here analyse such a model in a variational framework, particularly well suited for finite element applications. We are thus led to consider two uncoupled variational problems, namely the membranal and the bending one. The former one was independently formulated in Reference [7].

We recognize that the membranal problem is in fact elliptic, so that a standard finite element discretization properly works. As far as the bending problem is concerned, we first re-write the governing equation in such a way that they lead to a symmetric variational formulation. Furthermore, we recognize that we are dealing with a penalization of a constrained problem, the

*Correspondence to: C. Lovadina, Department of Mechanical and Structural Engineering, University of Trento, Via Mesiano 77, I-38050 Trento, Italy
†E-mail: lovadina@ing.unitn.it

Received 9 March 1999
Revised 9 November 1999

penalization parameter being essentially the plate thickness. We show that a suitable scaling for the electromechanical loads applied to the plate is capable to recover the Kirchhoff-type model proposed in Reference [11]. Moreover, a mixed formulation, arising from the introduction of the scaled shear stress as independent unknown, is presented. We then pass to discuss the discretization of the problem by means of finite element techniques. We mainly consider the case of bending behaviours, since, as already mentioned, the membranal problem has been recognized to be standard. In particular, a finite element method based on a *linking technique* (cf. References [12, 13]) is studied. The main result consists in establishing an error estimate which predicts the convergence of the proposed method when the mesh is refined, and uniform in the thickness. We finally present some numerical tests, showing the accordance of the computational performances with the theoretical predictions.

In Appendix A we establish a convergence result referred to in this paper. In Appendix B we report a brief derivation of the piezoelectric plate model proposed in Reference [10] and highlight the hypotheses on which it relies. In Appendix C we present a critical evaluation of this model, through an *analytical* comparison between the results it supplies and the ones supplied by the Voigt theory of piezoelectricity.

2. THE PIEZOELECTRIC PLATE MODEL

Let $A = \Omega \times (-t/2, t/2)$ be a plate-like region, with regular midplane $\Omega \subset \mathbb{R}^2$ and thickness $t > 0$. Let italic letters represent scalars, if not otherwise specified; bold italic letters denote elements of the two-dimensional vector space V parallel to Ω; and bold roman letters denote elements of the space Sym of second-order tensors over V.

The region A is the reference configuration of a plate comprised by a homogeneous linearly-piezoelectric transversely isotropic material (Hermann–Maugin class ∞mm [1]), with the axis of transverse isotropy oriented in the thickness direction. The constitutive behaviour of such a material is completely described by 10 independent material constants. By adopting a standard notation [1], the 'closed-circuit' elastic moduli are denoted by c_{11}, c_{33}, c_{44}, c_{12} and c_{13}; the 'clamped' permittivity constants are denoted by ε_{11} and ε_{33}; and the 'closed-circuit/clamped' piezoelectric constants are denoted by e_{31}, e_{33} and e_{15}. In order to guarantee a stable behaviour of the material, these constants are assumed to satisfy the inequalities $c_{11} > 0$, $|c_{12}| < c_{11}$, $2c_{13}^2 < c_{33}(c_{11} + c_{12})$, $\varepsilon_{33} > 0$, $c_{44} > 0$, $\varepsilon_{11} > 0$. For a later use, the following auxiliary material constants are introduced:

$$\begin{aligned}
\bar{\varepsilon}_{33} &= \varepsilon_{33} + e_{33}^2/c_{33} \\
\bar{\varepsilon}_{11} &= \varepsilon_{11} + e_{15}^2/c_{44} \\
\bar{e}_{31} &= e_{31} - c_{13}e_{33}/c_{33} \\
c_{66} &= (c_{11} - c_{12})/2 \\
\bar{c}_{11} &= c_{11} - c_{13}^2/c_{33} \\
\bar{c}_{12} &= c_{12} - c_{13}^2/c_{33} \\
\hat{c}_{11} &= \bar{c}_{11} + \bar{e}_{31}^2/\bar{\varepsilon}_{33} \\
\hat{c}_{12} &= \bar{c}_{12} + \bar{e}_{31}^2/\bar{\varepsilon}_{33}
\end{aligned} \tag{1}$$

The plate is acted upon on its upper and lower faces $\Omega \times \{\pm t/2\}$ by surface in-plane forces $\boldsymbol{P}^{\pm}$, surface normal forces $P^{\pm}$ and surface free electric charges $\Upsilon^{\pm}$. For the sake of simplicity, essentially without loss of generality, no body loads are considered and the plate is assumed to be clamped and grounded along its lateral boundary $\partial\Omega \times (-t/2, t/2)$.

It is of interest in applications to compute the displacement field, the electric potential field, the strain field, the stress field, the electric field, and the electric-displacement field which arise in the plate, due to the presence of the applied loads. According to the piezoelectric plate model proposed in Reference [10], these fields, which are of course defined over the three-dimensional region A, are parametrized by the unknown functions $\boldsymbol{U}$, W, $\boldsymbol{\Theta}$, Π and X, defined over the two-dimensional region Ω. For example, the in-plane displacement field $\boldsymbol{S}$, the transversal displacement field S and the electric potential field Φ are given by

$$\begin{aligned} \boldsymbol{S}(\boldsymbol{Y},\zeta) &= \boldsymbol{U}(\boldsymbol{Y}) + \zeta\boldsymbol{\Theta}(\boldsymbol{Y}) \\ S(\boldsymbol{Y},\zeta) &= W(\boldsymbol{Y}) \\ \Phi(\boldsymbol{Y},\zeta) &= \Pi(\boldsymbol{Y}) + \zeta X(\boldsymbol{Y}) \end{aligned} \tag{2}$$

where a Cartesian reference frame $(O, \boldsymbol{Y}, \zeta)$ is chosen with the origin O on the middle cross-section of the plate and the ζ-axis in the thickness direction. In particular, the meaning of the unknowns $\boldsymbol{U}$, W, $\boldsymbol{\Theta}$, Π, and X clearly appears: $\boldsymbol{U}$, W, and Π are, respectively, the in-plane displacement, the transversal displacement and the electric potential of the middle cross-section, $\boldsymbol{\Theta}$ is the rotation of the transversal fibres and $-X$ is the transversal electric field.

The unknown fields are determined by solving the following two uncoupled boundary-value problems [10]

$\mathscr{M}$—Membranal (or stretching, or in-plane) problem:
find $(\boldsymbol{U}, X)$ defined over Ω and satisfying the equations

$$\begin{aligned} -t\,\boldsymbol{div}\,(2c_{66}\boldsymbol{\nabla}^S\boldsymbol{U} + \bar{c}_{12}\mathbf{I}\,\mathrm{div}\,\boldsymbol{U}) - t\bar{e}_{31}\boldsymbol{\nabla}X &= \boldsymbol{R}^* \\ (t^3/12)\bar{\varepsilon}_{11}\Delta X + t[-\bar{\varepsilon}_{33}X + \bar{e}_{31}\,\mathrm{div}\,\boldsymbol{U}] &= -\Upsilon^* \end{aligned} \tag{3}$$

equipped with homogeneous Dirichlet boundary conditions;
$\mathscr{B}$—Bending (or transversal) problem:
find $(\boldsymbol{\Theta}, W, \Pi)$ defined over Ω and satisfying the equations

$$\begin{aligned} -(t^3/12)\boldsymbol{div}\,(2c_{66}\boldsymbol{\nabla}^S\boldsymbol{\Theta} + \hat{c}_{12}\,\mathbf{I}\,\mathrm{div}\,\boldsymbol{\Theta}) + t[c_{44}(\boldsymbol{\Theta} + \boldsymbol{\nabla}W) + e_{15}\boldsymbol{\nabla}\Pi] &= \boldsymbol{M}^* \\ -t\,\mathrm{div}\,[c_{44}(\boldsymbol{\Theta} + \boldsymbol{\nabla}W) + e_{15}\boldsymbol{\nabla}\Pi] &= R^* \\ -t\,\mathrm{div}\,[-\varepsilon_{11}\boldsymbol{\nabla}\Pi + e_{15}(\boldsymbol{\Theta} + \boldsymbol{\nabla}W)] &= -\Psi^* \end{aligned} \tag{4}$$

equipped with homogeneous Dirichlet boundary conditions.

In Equations (3) and (4), div denotes the divergence operator acting on vector fields, ***div*** denotes the divergence operator acting on tensor fields, $\boldsymbol{\nabla}$ denotes the gradient operator acting on scalar fields, $\boldsymbol{\nabla}^S$ denotes the symmetric part of the gradient operator acting on vector fields, Δ denotes

the Laplace operator acting on scalar fields and $\mathbf{I}$ is the unit second-order tensor over V. Moreover,

$$\begin{aligned} \boldsymbol{R}^* &= \boldsymbol{P}^+ + \boldsymbol{P}^- \\ \Upsilon^* &= (t/2)(\Upsilon^+ - \Upsilon^-) \\ \boldsymbol{M}^* &= (t/2)(\boldsymbol{P}^+ - \boldsymbol{P}^-) \\ R^* &= P^+ + P^- \\ \Psi^* &= \Upsilon^+ + \Upsilon^- \end{aligned} \tag{5}$$

It is pointed out that the applied loads enter Equations (3) and (4) only through the quantities $\boldsymbol{R}^*$, Υ^*, $\boldsymbol{M}^*$, R^* and Ψ^*. For this reason, in what follows just these quantities (instead of $\boldsymbol{P}^\pm$, $P^\pm$ and $\Upsilon^\pm$) will be regarded as data. Moreover, we will always suppose them to be smooth enough, namely L^2-regular.

2.1. The membranal problem

Following the guideline used for elastic plate problems [14], a sequence of problems, capable to lead to a good limit problem as the thickness approaches zero, is introduced. More precisely, the electro-mechanical loads are scaled in such a way to recover, at the limit $t \to 0$, the Kirchhoff-type piezoelectric model proposed in Reference [11]. The following positions are thus introduced:

$$\begin{aligned} \boldsymbol{R}^* &= t\boldsymbol{R} \\ \Upsilon^* &= t\Upsilon \end{aligned} \tag{6}$$

where $\boldsymbol{R}$ and Υ are independent of t.

Moreover, for the sake of simplicity, dimensionless quantities are introduced

$$\begin{aligned} \boldsymbol{u} &= \boldsymbol{U}/l \\ \chi &= X\sqrt{\bar{\varepsilon}_{33}/\bar{c}_{11}} \\ \boldsymbol{r} &= \boldsymbol{R}l/\bar{c}_{11} \\ \upsilon &= \Upsilon/\sqrt{\bar{\varepsilon}_{33}\bar{c}_{11}} \end{aligned} \tag{7}$$

where l is a characteristic in-plane length (e.g. the diameter of Ω). In addition, the following dimensionless material constants are defined:

$$\begin{aligned} \nu &= \bar{c}_{12}/\bar{c}_{11} \\ \alpha &= \sqrt{\bar{\varepsilon}_{11}/(12\bar{\varepsilon}_{33})} \\ \xi &= \bar{e}_{31}/\sqrt{\bar{c}_{11}\bar{\varepsilon}_{33}} \end{aligned} \tag{8}$$

and the slenderness (small) parameter δ is defined as follows:

$$\delta = \alpha\frac{t}{l} \tag{9}$$

It is easily seen that the membranal problem $\mathscr{M}$ is equivalent to the following system.

- Find $(\boldsymbol{u}, \chi)$, solution of

$$\begin{aligned} -\boldsymbol{div}\left((1-\nu)\boldsymbol{\nabla}^S\boldsymbol{u} + \nu\mathbf{I}\,\mathrm{div}\,\boldsymbol{u}\right) - \xi\boldsymbol{\nabla}\chi &= \boldsymbol{r} \\ \xi\,\mathrm{div}\,\boldsymbol{u} - \chi + \delta^2\Delta\chi &= -\upsilon \end{aligned} \tag{10}$$

equipped with homogeneous Dirichlet boundary conditions. Here and in the remainder of this section differential operators are intended with respect to the dimensionless in-plane variable $\boldsymbol{y} = \boldsymbol{Y}/l$, which range in the domain $\omega = \{\boldsymbol{y}\colon l\boldsymbol{y} \in \Omega\}$.

A classical functional framework is chosen for problem (10). In particular, let $(\cdot,\cdot)$ denote the scalar product in $L^2(\omega)$; $||\cdot||_0$ the $L^2(\omega)$-norm, $||\cdot||_1$ the $H_0^1(\omega)$-norm and $|\cdot|_1$ the seminorm defined as the $L^2(\omega)$-norm of the gradient of the argument. Then, problem (10) is recasted into the variational formulation

- Find $(\boldsymbol{u},\chi) \in H_0^1(\omega)^2 \times H_0^1(\omega)$, solution of

$$\begin{aligned}(1-\nu)(\boldsymbol{\nabla}^S\boldsymbol{u},\boldsymbol{\nabla}^S\boldsymbol{v}) + \nu(\operatorname{div}\boldsymbol{u},\operatorname{div}\boldsymbol{v}) + \xi(\chi,\operatorname{div}\boldsymbol{v}) &= (\boldsymbol{r},\boldsymbol{v}) \quad \forall \boldsymbol{v} \in H_0^1(\omega)^2\\ \xi(\operatorname{div}\boldsymbol{u},\tau) - (\chi,\tau) - \delta^2(\boldsymbol{\nabla}\chi,\boldsymbol{\nabla}\tau) &= -(\upsilon,\tau) \quad \forall \tau \in H_0^1(\omega)\end{aligned} \tag{11}$$

The following result establishes the uniform boundedness of the family of solutions $(\boldsymbol{u},\chi)$, as δ approaches zero, in the space $H_0^1(\omega)^2 \times L^2(\omega)$.

Proposition 2.1. System (11) has a unique solution $(\boldsymbol{u},\chi) \in H_0^1(\omega)^2 \times H_0^1(\omega)$. Moreover, the following estimate holds

$$||\boldsymbol{u}||_1 + ||\chi||_0 + \delta|\chi|_1 \leqslant C \tag{12}$$

Proof: Let

$$\begin{aligned}\mathscr{A}_{\mathscr{M}}(\boldsymbol{u},\chi;\boldsymbol{v},\tau) := (1-\nu)(\boldsymbol{\nabla}^S\boldsymbol{u},\boldsymbol{\nabla}^S\boldsymbol{v}) + \nu(\operatorname{div}\boldsymbol{u},\operatorname{div}\boldsymbol{v}) + \xi(\chi,\operatorname{div}\boldsymbol{v})\\ -\xi(\operatorname{div}\boldsymbol{u},\tau) + (\chi,\tau) + \delta^2(\boldsymbol{\nabla}\chi,\boldsymbol{\nabla}\tau)\end{aligned} \tag{13}$$

It is easily recognized that problem (11) is equivalent to the following problem.

- Find $(\boldsymbol{u},\chi) \in H_0^1(\omega)^2 \times H_0^1(\omega)$, solution of

$$\mathscr{A}_{\mathscr{M}}(\boldsymbol{u},\chi;\boldsymbol{v},\tau) = (\boldsymbol{r},\boldsymbol{v}) + (\upsilon,\tau) \quad \forall (\boldsymbol{v},\tau) \in H_0^1(\omega)^2 \times H_0^1(\omega) \tag{14}$$

The space $H_0^1(\omega)^2 \times H_0^1(\omega)$ is then endowed with the norm

$$|||\boldsymbol{u},\chi|||^2 := ||\boldsymbol{u}||_1^2 + ||\chi||_0^2 + \delta^2|\chi|_1^2 \tag{15}$$

with respect to which $\mathscr{A}_{\mathscr{M}}$ is bounded:

$$\mathscr{A}_{\mathscr{M}}(\boldsymbol{u},\chi;\boldsymbol{v},\tau) \leqslant C|||\boldsymbol{u},\chi|||\,|||\boldsymbol{v},\tau||| \tag{16}$$

In addition, since $|\nu| < 1$, $\mathscr{A}_{\mathscr{M}}$ is also coercive with respect to the $|||\cdot|||$-norm, as a consequence of Korn's inequality:

$$\mathscr{A}_{\mathscr{M}}(\boldsymbol{u},\chi;\boldsymbol{u},\chi) \geqslant C|||\boldsymbol{u},\chi|||^2 \quad \forall (\boldsymbol{u},\chi) \in H_0^1(\omega)^2 \times H_0^1(\omega) \tag{17}$$

Hence, by the Lax–Milgram lemma it follows that problem (14) has a unique solution. Estimate (12) is an easy consequence of the standard theory. □

Furthermore, by using estimate (12), the following proposition follows.

Proposition 2.2. The couple $(\boldsymbol{u}, \chi)$ strongly converges in $H_0^1(\omega)^2 \times L^2(\omega)$, as $\delta \to 0$, to $(\boldsymbol{u}_0, \chi_0) \in H_0^1(\omega)^2 \times L^2(\omega)$, solution of the variational problem

- Find $(\boldsymbol{u}_0, \chi_0) \in H_0^1(\omega)^2 \times L^2(\omega)$, such that

$$\begin{aligned} (1-\nu)(\boldsymbol{\nabla}^S \boldsymbol{u}_0, \boldsymbol{\nabla}^S \boldsymbol{v}) + \nu(\operatorname{div} \boldsymbol{u}_0, \operatorname{div} \boldsymbol{v}) + \xi(\chi_0, \operatorname{div} \boldsymbol{v}) &= (\boldsymbol{r}, \boldsymbol{v}) \quad \forall \boldsymbol{v} \in H_0^1(\omega)^2 \\ \xi(\operatorname{div} \boldsymbol{u}_0, \tau) - (\chi_0, \tau) &= -(\upsilon, \tau) \quad \forall \tau \in L^2(\omega) \end{aligned} \tag{18}$$

Remark 2.1. It is remarked that problem (18), in differential form, reads as follows:

- Find $(\boldsymbol{u}_0, \chi_0)$, solution of

$$\begin{aligned} -\boldsymbol{div}\,((1-\nu)\boldsymbol{\nabla}^S \boldsymbol{u}_0 + \nu \mathbf{I} \operatorname{div} \boldsymbol{u}_0) - \xi \boldsymbol{\nabla} \chi_0 &= \boldsymbol{r} \\ \xi \operatorname{div} \boldsymbol{u}_0 - \chi_0 &= -\upsilon \end{aligned} \tag{19}$$

which is just the limit of the system (10) as δ approaches zero. In particular, $\boldsymbol{u}_0$ solves the differential equation in Ω

$$-\boldsymbol{div}\,((1-\nu)\boldsymbol{\nabla}^S \boldsymbol{u}_0 + \nu \mathbf{I} \operatorname{div} \boldsymbol{u}_0) - \xi^2 \boldsymbol{\nabla} \operatorname{div} \boldsymbol{u}_0 = \boldsymbol{r} + \xi \boldsymbol{\nabla} \upsilon \tag{20}$$

and χ_0 is then post-computed by the equation

$$\chi_0 = \xi \operatorname{div} \boldsymbol{u}_0 + \upsilon \tag{21}$$

Of course, no boundary conditions can be imposed on χ_0 in the limit problem. We remark that the loss of boundary conditions for χ_0 causes, in general, a boundary layer effect. The study of such phenomenon, altough very interesting, is not investigated in the present paper.

The above equations fit the framework of the Kirchhoff-type piezoelectric plate theory recently proposed by Bisegna and Maceri (cf. Reference [11]). More precisely, it is the governing equation for the in-plane mechanical equilibrium.

Remark 2.2. It is pointed out that the membranal piezoelectric problem is essentially an elliptic problem, so that standard finite elements should properly work and no pathological phenomena such as locking effects should occur.

2.2. The bending problem

As in the previous case, the electromechanical loads are scaled in such a way to recover, at the limit $t \to 0$, the Kirchhoff-type piezoelectric model proposed in Reference [11]. The following positions are thus introduced:

$$\begin{aligned} \boldsymbol{M}^* &= t^3 \boldsymbol{M} \\ R^* &= t^3 R \\ \Psi^* &= t \Psi \end{aligned} \tag{22}$$

where $\boldsymbol{M}$, R and Ψ are independent of t.

In addition, the following dimensionless quantities are defined:

$$\begin{aligned} \boldsymbol{\theta} &= \boldsymbol{\Theta} \\ w &= W/l \\ \beta &= (\Pi/l)\sqrt{\bar{\varepsilon}_{11}/c_{44}} \\ \boldsymbol{m} &= 12\boldsymbol{M}l^2/\hat{c}_{11} \\ r &= 12Rl^3/\hat{c}_{11} \\ \psi &= \Psi l/\sqrt{c_{44}\bar{\varepsilon}_{11}} \end{aligned} \tag{23}$$

together with some dimensionless material constants

$$\begin{aligned} \mu &= \hat{c}_{12}/\hat{c}_{11} \\ \lambda &= \sqrt{\hat{c}_{11}/(12c_{44})} \\ \kappa &= e_{15}/\sqrt{c_{44}\bar{\varepsilon}_{11}} \end{aligned} \tag{24}$$

and the following slenderness (small) parameter ε

$$\varepsilon = \lambda\frac{t}{l} \tag{25}$$

It is easily seen that the bending problem $\mathscr{B}$ is equivalent to the following system.

- Find $(\boldsymbol{\theta}, w, \beta)$, solution of

$$\begin{aligned} -\boldsymbol{div}\,((1-\mu)\boldsymbol{\nabla}^S\boldsymbol{\theta} + \mu\mathbf{I}\,\mathrm{div}\,\boldsymbol{\theta}) + \varepsilon^{-2}[\boldsymbol{\theta} + \boldsymbol{\nabla}w + \kappa\boldsymbol{\nabla}\beta] &= \boldsymbol{m} \\ -\varepsilon^{-2}\,\mathrm{div}[\boldsymbol{\theta} + \boldsymbol{\nabla}w + \kappa\boldsymbol{\nabla}\beta] &= r \\ \Delta\beta - \kappa\,\mathrm{div}(\boldsymbol{\theta} + \boldsymbol{\nabla}w + \kappa\boldsymbol{\nabla}\beta) &= -\psi \end{aligned} \tag{26}$$

equipped with homogeneous Dirichlet boundary conditions.

Here and in the remainder of this section differential operators are intended with respect to the dimensionless variable $\boldsymbol{y}$. Moreover, let us notice that for $\kappa = 0$ problem (26) turns out to be the usual purely elastic plate problem. Thus, in the sequel we will only consider the case $\kappa \neq 0$. This system is then recasted in a variational formulation as follows.

- Find $(\boldsymbol{\theta}, w, \beta) \in H_0^1(\omega)^2 \times H_0^1(\omega) \times H_0^1(\omega)$, solution of

$$\begin{aligned} a_{\mathscr{B}}(\boldsymbol{\theta}, \boldsymbol{\eta}) + \varepsilon^{-2}(\boldsymbol{\theta} + \boldsymbol{\nabla}w + \kappa\boldsymbol{\nabla}\beta, \boldsymbol{\eta}) &= (\boldsymbol{m}, \boldsymbol{\eta}) \quad \forall \boldsymbol{\eta} \in H_0^1(\omega)^2 \\ \varepsilon^{-2}(\boldsymbol{\theta} + \boldsymbol{\nabla}w + \kappa\boldsymbol{\nabla}\beta, \boldsymbol{\nabla}\zeta) &= (r, \zeta) \quad \forall \zeta \in H_0^1(\omega) \\ -(\boldsymbol{\nabla}\beta, \boldsymbol{\nabla}\rho) + \kappa(\boldsymbol{\theta} + \boldsymbol{\nabla}w + \kappa\boldsymbol{\nabla}\beta, \boldsymbol{\nabla}\rho) &= -(\psi, \rho) \quad \forall \rho \in H_0^1(\omega) \end{aligned} \tag{27}$$

where

$$a_{\mathscr{B}}(\boldsymbol{\theta},\boldsymbol{\eta}) := ((1-\mu)\boldsymbol{\nabla}^S\boldsymbol{\theta},\boldsymbol{\nabla}^S\boldsymbol{\eta}) + (\mu\,\mathrm{div}\,\boldsymbol{\theta},\mathrm{div}\,\boldsymbol{\eta}) \tag{28}$$

A glance at it reveals that a first drawback stands in its lack of symmetry. In order to find out an equivalent variational formulation overcoming this difficulty, the third equation of (26) is modified. It is multiplied by -1 and the result is added with the second of (26) multiplied by $(1+\varepsilon^2)\kappa$. Then, the differential problem (26) has been changed into the following problem.

- Find $(\boldsymbol{\theta}, w, \beta)$, solution of

$$\begin{aligned} -\boldsymbol{div}\,((1-\mu)\boldsymbol{\nabla}^S\boldsymbol{\theta} + \mu\mathbf{I}\,\mathrm{div}\,\boldsymbol{\theta}) + \varepsilon^{-2}[\boldsymbol{\theta} + \boldsymbol{\nabla}w + \kappa\boldsymbol{\nabla}\beta] &= \boldsymbol{m} \\ -\varepsilon^{-2}\,\mathrm{div}[\boldsymbol{\theta} + \boldsymbol{\nabla}w + \kappa\boldsymbol{\nabla}\beta] &= r \\ -\Delta\beta - \kappa\varepsilon^{-2}\,\mathrm{div}(\boldsymbol{\theta} + \boldsymbol{\nabla}w + \kappa\boldsymbol{\nabla}\beta) &= \psi + \kappa(1+\varepsilon^2)r \end{aligned} \tag{29}$$

equipped with homogeneous Dirichlet boundary conditions.

Trivially, the following proposition holds.

Proposition 2.3. The two problems (26) and (29) are equivalent.

A variational formulation of problem (29) reads as follows:

- Find $(\boldsymbol{\theta}, w, \beta) \in H_0^1(\omega)^2 \times H_0^1(\omega) \times H_0^1(\omega)$, solution of

$$\begin{aligned} a_{\mathscr{B}}(\boldsymbol{\theta},\boldsymbol{\eta}) + \varepsilon^{-2}(\boldsymbol{\theta} + \boldsymbol{\nabla}w + \kappa\boldsymbol{\nabla}\beta,\boldsymbol{\eta}) &= (\boldsymbol{m},\boldsymbol{\eta}) \quad \forall\boldsymbol{\eta}\in H_0^1(\omega)^2 \\ \varepsilon^{-2}(\boldsymbol{\theta} + \boldsymbol{\nabla}w + \kappa\boldsymbol{\nabla}\beta, \boldsymbol{\nabla}\zeta) &= (r,\zeta) \quad \forall\zeta\in H_0^1(\omega) \\ (\boldsymbol{\nabla}\beta,\boldsymbol{\nabla}\rho) + \varepsilon^{-2}(\boldsymbol{\theta} + \boldsymbol{\nabla}w + \kappa\boldsymbol{\nabla}\beta,\kappa\boldsymbol{\nabla}\rho) &= (\psi,\rho) + \kappa(1+\varepsilon^2)(r,\rho) \quad \forall\rho\in H_0^1(\omega) \end{aligned} \tag{30}$$

Let us set

$$\mathscr{A}_\varepsilon(\boldsymbol{\theta},w,\beta;\boldsymbol{\eta},\zeta,\rho) := \mathscr{A}_{\mathscr{B}}(\boldsymbol{\theta},w,\beta;\boldsymbol{\eta},\zeta,\rho) + \varepsilon^{-2}\mathscr{A}_S(\boldsymbol{\theta},w,\beta;\boldsymbol{\eta},\zeta,\rho) \tag{31}$$

where

$$\mathscr{A}_{\mathscr{B}}(\boldsymbol{\theta},w,\beta;\boldsymbol{\eta},\zeta,\rho) := a_{\mathscr{B}}(\boldsymbol{\theta},\boldsymbol{\eta}) + (\boldsymbol{\nabla}\beta,\boldsymbol{\nabla}\rho) \tag{32}$$

and

$$\mathscr{A}_S(\boldsymbol{\theta},w,\beta;\boldsymbol{\eta},\zeta,\rho) := (\boldsymbol{\theta} + \boldsymbol{\nabla}w + \kappa\boldsymbol{\nabla}\beta, \boldsymbol{\eta} + \boldsymbol{\nabla}\zeta + \kappa\boldsymbol{\nabla}\rho) \tag{33}$$

and

$$\mathscr{L}_\varepsilon(\boldsymbol{\eta},\zeta,\rho) := (\boldsymbol{m},\boldsymbol{\eta}) + (r,\zeta) + (\psi,\rho) + \varepsilon^2\kappa(r,\rho) + \kappa(r,\rho) \tag{34}$$

It is easily recognized that the variational problem (29) may be written as

- Find $(\boldsymbol{\theta}, w, \beta) \in H_0^1(\omega)^2 \times H_0^1(\omega) \times H_0^1(\omega)$, solution of

$$\mathscr{A}_\varepsilon(\boldsymbol{\theta},w,\beta;\boldsymbol{\eta},\zeta,\rho) = \mathscr{L}_\varepsilon(\boldsymbol{\eta},\zeta,\rho) \quad \forall(\boldsymbol{\eta},\zeta,\rho)\in H_0^1(\omega)^2 \times H_0^1(\omega) \times H_0^1(\omega) \tag{35}$$

In order to understand the behaviour of the solution $(\boldsymbol{\theta}, w, \beta)$ as the parameter ε approaches zero, the subspace $\mathscr{K} \subset H_0^1(\omega)^2 \times H_0^1(\omega) \times H_0^1(\omega)$ is defined by

$$\mathscr{K} = \{(\boldsymbol{\eta}, \zeta, \rho) \in H_0^1(\omega)^2 \times H_0^1(\omega) \times H_0^1(\omega) : \boldsymbol{\eta} + \boldsymbol{\nabla}(\zeta + \kappa\rho) = 0\} \tag{36}$$

i.e. $\mathscr{K}$ is the kernel of the continuous bilinear form $\mathscr{A}_S$ (cf. (33)). Due to the continuity, $\mathscr{K}$ is a closed subspace of $H_0^1(\omega)^2 \times H_0^1(\omega) \times H_0^1(\omega)$. Furthermore, it is straightforward to check that $\mathscr{K} \neq (0)$.

First, the following lemma is proved.

Lemma 2.1. The bilinear form $\mathscr{A}_{\mathscr{B}}$ defined by (32) is coercive over the subspace $\mathscr{K}$.

Proof: Let $(\boldsymbol{\eta}, \zeta, \rho) \in \mathscr{K}$. By Korn's inequality

$$\mathscr{A}_{\mathscr{B}}(\boldsymbol{\eta}, \zeta, \rho; \boldsymbol{\eta}, \zeta, \rho) = a_{\mathscr{B}}(\boldsymbol{\eta}, \boldsymbol{\eta}) + ||\boldsymbol{\nabla}\rho||_0^2 \geqslant \frac{C}{2}||\boldsymbol{\eta}||_1^2 + \frac{C}{2}||\boldsymbol{\eta}||_1^2 + ||\boldsymbol{\nabla}\rho||_0^2 \tag{37}$$

Since $(\boldsymbol{\eta}, \zeta, \rho) \in \mathscr{K}$ it holds

$$\boldsymbol{\eta} + \boldsymbol{\nabla}(\zeta + \kappa\rho) = 0 \tag{38}$$

by which

$$||\boldsymbol{\eta}||_1^2 \geqslant ||\boldsymbol{\eta}||_0^2 = ||\boldsymbol{\nabla}(\zeta + \kappa\rho)||_0^2 \tag{39}$$

Hence

$$\mathscr{A}_{\mathscr{B}}(\boldsymbol{\eta}, \zeta, \rho; \boldsymbol{\eta}, \zeta, \rho) \geqslant \frac{C}{2}||\boldsymbol{\eta}||_1^2 + \frac{C}{2}||\boldsymbol{\nabla}(\zeta + \kappa\rho)||_0^2 + ||\boldsymbol{\nabla}\rho||_0^2 \tag{40}$$

and the estimate

$$\mathscr{A}_{\mathscr{B}}(\boldsymbol{\eta}, \zeta, \rho; \boldsymbol{\eta}, \zeta, \rho) \geqslant C(||\boldsymbol{\eta}||_1^2 + ||\zeta||_1^2 + ||\rho||_1^2) \tag{41}$$

follows by a little algebra along with Poincaré's inequality. The proof is thus complete. □

Now it is not difficult to prove the proposition.

Proposition 2.4. Let $(\boldsymbol{\theta}, w, \beta)$ be the solution of variational problem (35). Then $(\boldsymbol{\theta}, w, \beta)$ strongly converges, as ε approaches zero, to $(\boldsymbol{\theta}_0, w_0, \beta_0) \in \mathscr{K}$, solution of the following problem.

- Find $(\boldsymbol{\theta}_0, w_0, \beta_0) \in \mathscr{K}$, solution of

$$\mathscr{A}_{\mathscr{B}}(\boldsymbol{\theta}_0, w_0, \beta_0; \boldsymbol{\eta}_0, \zeta_0, \rho_0) = \mathscr{L}_0(\boldsymbol{\eta}_0, \zeta_0, \rho_0) \quad \forall (\boldsymbol{\eta}_0, \zeta_0, \rho_0) \in \mathscr{K} \tag{42}$$

where $\mathscr{L}_0$ is defined by

$$\mathscr{L}_0(\boldsymbol{\eta}, \zeta, \rho) := (\boldsymbol{m}, \boldsymbol{\eta}) + (r, \zeta) + (\psi, \rho) + \kappa(r, \rho) \tag{43}$$

Moreover, $(\boldsymbol{\theta}_0, w_0, \beta_0) = 0$ if and only if $\mathscr{L}_0 \in \mathscr{K}^0$, $\mathscr{K}^0$ being the polar set of $\mathscr{K}$.

Proof: As it is straightforward to check that $\mathscr{L}_\varepsilon$ strongly converges to $\mathscr{L}_0$, the proof is a direct consequence of the abstract result given in the appendix, together with Lemma 2.1. □

Proposition 2.4 says that problem (35) is nothing but a penalization of the *constrained* limit problem (42). This suggests to pass to a mixed formulation of the problem. More precisely, we set

$$\boldsymbol{\gamma} = \varepsilon^{-2}(\boldsymbol{\theta} + \boldsymbol{\nabla}w + \kappa\boldsymbol{\nabla}\beta) \tag{44}$$

as Lagrange multiplier, and we get in a standard way the following mixed variational formulation of the problem.

- Find $(\boldsymbol{\theta}, w, \beta; \boldsymbol{\gamma}) \in H_0^1(\omega)^2 \times H_0^1(\omega) \times H_0^1(\omega) \times L^2(\omega)^2$, solution of

$$\begin{aligned} a_{\mathscr{B}}(\boldsymbol{\theta}, \boldsymbol{\eta}) + (\boldsymbol{\nabla}\beta, \boldsymbol{\nabla}\rho) + (\boldsymbol{\gamma}, \boldsymbol{\eta} + \boldsymbol{\nabla}\zeta + \kappa\boldsymbol{\nabla}\rho) &= (\boldsymbol{m}, \boldsymbol{\eta}) + (r, \zeta) + (\psi, \rho) + \kappa(1+\varepsilon^2)(r, \rho) \\ (\boldsymbol{\theta} + \boldsymbol{\nabla}w + \kappa\boldsymbol{\nabla}\beta, \boldsymbol{s}) - \varepsilon^2(\boldsymbol{\gamma}, \boldsymbol{s}) &= 0 \end{aligned} \tag{45}$$

for each $(\boldsymbol{\eta}, \zeta, \rho, \boldsymbol{s}) \in H_0^1(\omega)^2 \times H_0^1(\omega) \times H_0^1(\omega) \times L^2(\omega)^2$

For problem (45) we have the following.

Proposition 2.5. Problem (45) has a unique solution $(\boldsymbol{\theta}, w, \beta; \boldsymbol{\gamma}) \in H_0^1(\omega)^2 \times H_0^1(\omega) \times H_0^1(\omega) \times L^2(\omega)^2$. Moreover, as $\varepsilon \to 0$, $(\boldsymbol{\theta}, w, \beta; \boldsymbol{\gamma})$ converges to $(\boldsymbol{\theta}_0, w_0, \beta_0; \boldsymbol{\gamma}_0)$ in $H_0^1(\omega)^2 \times H_0^1(\omega) \times H_0^1(\omega) \times H^{-1}(\mathrm{div}, \omega)$, where $(\boldsymbol{\theta}_0, w_0, \beta_0; \boldsymbol{\gamma}_0)$ is the solution of the problem

- Find $(\boldsymbol{\theta}_0, w_0, \beta_0; \boldsymbol{\gamma}_0) \in H_0^1(\omega)^2 \times H_0^1(\omega) \times H_0^1(\omega) \times H^{-1}(\mathrm{div}, \omega)$, solution of

$$\begin{aligned} a_{\mathscr{B}}(\boldsymbol{\theta}_0, \boldsymbol{\eta}) + (\boldsymbol{\nabla}\beta_0, \boldsymbol{\nabla}\rho) + (\boldsymbol{\gamma}_0, \boldsymbol{\eta} + \boldsymbol{\nabla}\zeta + \kappa\boldsymbol{\nabla}\rho) &= (\boldsymbol{m}, \boldsymbol{\eta}) + (r, \zeta) + (\psi, \rho) + \kappa(r, \rho) \\ (\boldsymbol{\theta}_0 + \boldsymbol{\nabla}w_0 + \kappa\boldsymbol{\nabla}\beta_0, \boldsymbol{s}) &= 0 \end{aligned} \tag{46}$$

for each $(\boldsymbol{\eta}, \zeta, \rho, \boldsymbol{s}) \in H_0^1(\omega)^2 \times H_0^1(\omega) \times H_0^1(\omega) \times H^{-1}(\mathrm{div}, \omega)$.

Above, $H^{-1}(\mathrm{div}, \omega)$ is the Hilbert space defined by

$$H^{-1}(\mathrm{div}, \omega) := \{\boldsymbol{s} \in H^{-1}(\omega)^2 : \ \mathrm{div}\, \boldsymbol{s} \in H^{-1}(\omega)\} \tag{47}$$

equipped with the norm

$$||\boldsymbol{s}||^2_{H^{-1}(\mathrm{div}, \omega)} := ||\boldsymbol{s}||^2_{-1} + ||\mathrm{div}\, \boldsymbol{s}||^2_{-1} \tag{48}$$

Setting

$$\mathscr{A}(\boldsymbol{\theta}, w, \beta, \boldsymbol{\gamma}; \boldsymbol{\eta}, \zeta, \rho) = a_{\mathscr{B}}(\boldsymbol{\theta}, \boldsymbol{\eta}) + (\boldsymbol{\nabla}\beta, \boldsymbol{\nabla}\rho) + (\boldsymbol{\gamma}, \boldsymbol{\eta} + \boldsymbol{\nabla}\zeta + \kappa\boldsymbol{\nabla}\rho) - (\boldsymbol{\theta} + \boldsymbol{\nabla}w + \kappa\boldsymbol{\nabla}\beta, \boldsymbol{s}) + \varepsilon^2(\boldsymbol{\gamma}, \boldsymbol{s}) \tag{49}$$

our mixed problem can also be written as

- Find $(\boldsymbol{\theta}, w, \beta; \boldsymbol{\gamma}) \in H_0^1(\omega)^2 \times H_0^1(\omega) \times H_0^1(\omega) \times L^2(\omega)^2$, solution of

$$\mathscr{A}(\boldsymbol{\theta}, w, \beta, \boldsymbol{\gamma}; \boldsymbol{\eta}, \zeta, \rho, \boldsymbol{s}) = \mathscr{L}_\varepsilon(\boldsymbol{\eta}, \zeta, \rho, \boldsymbol{s}) \quad \forall (\boldsymbol{\eta}, \zeta, \rho, \boldsymbol{s}) \in H_0^1(\omega)^2 \times H_0^1(\omega) \times H_0^1(\omega) \times L^2(\omega)^2 \tag{50}$$

where

$$\mathscr{L}_\varepsilon(\boldsymbol{\eta}, \zeta, \rho, \boldsymbol{s}) := \mathscr{L}_\varepsilon(\boldsymbol{\eta}, \zeta, \rho) \tag{51}$$

3. DISCRETIZATION OF THE PROBLEM

Aim of this section is to discuss the discretization of the piezoelectric problem by means of finite element techniques (cf. References [14, 15], for instance). As established in the previous section, we know that we are dealing with two uncoupled problems, so that we will treat them separately. Moreover, in what follows, we will suppose that our computational domain ω is partitioned by means of a sequence of quadrilateral regular meshes $\mathcal{T}_h$, where h represents the mesh size.

3.1. The discretized membranal problem

We notice that the membranal problem is essentially an ellptic problem, so that a standard discretization will lead to performant results. Thus, choosing $U_h \subset H_0^1(\Omega)^2$ and $X_h \subset H_0^1(\Omega)$ conforming finite element spaces, we consider the problem

- Find $(\boldsymbol{u}_h, \chi_h) \in U_h \times X_h$, solution of

$$\begin{aligned}(1-\nu)(\boldsymbol{\nabla}^S \boldsymbol{u}_h, \boldsymbol{\nabla}^S \boldsymbol{v}) + \nu(\operatorname{div} \boldsymbol{u}_h, \operatorname{div} \boldsymbol{v}) + \xi(\chi_h, \operatorname{div} \boldsymbol{v}) &= (\boldsymbol{r}, \boldsymbol{v}) \quad \forall \boldsymbol{v} \in U_h \\ \xi(\operatorname{div} \boldsymbol{u}_h, \tau) - (\chi_h, \tau) - \delta^2(\boldsymbol{\nabla}\chi_h, \boldsymbol{\nabla}\tau) &= -(\upsilon, \tau) \quad \forall \tau \in X_h\end{aligned} \tag{52}$$

For such a problem standard techniques for error analysis give the following.

Proposition 3.1. System (52) has a unique solution $(\boldsymbol{u}_h, \chi_h) \in U_h \times X_h$. Moreover, the following estimate holds:

$$||\boldsymbol{u} - \boldsymbol{u}_h||_1 + ||\chi - \chi_h||_0 + \delta|\chi - \chi_h|_1 \leqslant C \left(\inf_{\boldsymbol{v}_h \in U_h} ||\boldsymbol{u} - \boldsymbol{v}_h||_1 + \inf_{\tau_h \in X_h} (||\chi - \tau_h||_0 + \delta|\chi - \tau_h|_1) \right) \tag{53}$$

where $(\boldsymbol{u}, \chi)$ is the solution of problem (11).

For example, if we choose both $U_h \subset H_0^1(\omega)$ and $X_h \subset H_0^1(\omega)$ as the classical isoparametric bilinear finite element space, we have the following error estimate.

Corollary 3.1. Let $(\boldsymbol{u}_h, \chi_h) \in U_h \times X_h$ be the solution of system (52). It holds

$$||\boldsymbol{u} - \boldsymbol{u}_h||_1 + ||\chi - \chi_h||_0 + \delta|\chi - \chi_h|_1 \leqslant Ch \tag{54}$$

where $(\boldsymbol{u}, \chi)$ is the solution of problem (11).

3.2. The discretized bending problem

In this section we will deal with formulation (30) as the starting point of our discretization. Therefore, we here recall that we are considering the variational problem

- Find $(\boldsymbol{\theta}, w, \beta) \in H_0^1(\omega)^2 \times H_0^1(\omega) \times H_0^1(\omega)$, solution of

$$\begin{aligned}a_{\mathscr{B}}(\boldsymbol{\theta}, \boldsymbol{\eta}) + \varepsilon^{-2}(\boldsymbol{\theta} + \boldsymbol{\nabla} w + \kappa \boldsymbol{\nabla}\beta, \boldsymbol{\eta}) &= (\boldsymbol{m}, \boldsymbol{\eta}) \quad \forall \boldsymbol{\eta} \in H_0^1(\omega)^2 \\ \varepsilon^{-2}(\boldsymbol{\theta} + \boldsymbol{\nabla} w + \kappa \boldsymbol{\nabla}\beta, \boldsymbol{\nabla}\zeta) &= (r, \zeta) \quad \forall \zeta \in H_0^1(\omega) \\ (\boldsymbol{\nabla}\beta, \boldsymbol{\nabla}\rho) + \varepsilon^{-2}(\boldsymbol{\theta} + \boldsymbol{\nabla} w + \kappa \boldsymbol{\nabla}\beta, \kappa \boldsymbol{\nabla}\rho) &= (\psi, \rho) + \kappa(1+\varepsilon^2)(r, \rho) \quad \forall \rho \in H_0^1(\omega)\end{aligned} \tag{55}$$

which can also be written as (cf. (31)–(35))

- Find $(\boldsymbol{\theta}, w, \beta) \in H_0^1(\omega)^2 \times H_0^1(\omega) \times H_0^1(\omega)$, solution of

$$\mathscr{A}_{\mathscr{B}}(\boldsymbol{\theta}, w, \beta; \boldsymbol{\eta}, \zeta, \rho) + \varepsilon^{-2} \mathscr{A}_S(\boldsymbol{\theta}, w, \beta; \boldsymbol{\eta}, \zeta, \rho) = \mathscr{L}_\varepsilon(\boldsymbol{\eta}, \zeta, \rho) \tag{56}$$

for each $(\boldsymbol{\eta}, \zeta, \rho) \in H_0^1(\omega)^2 \times H_0^1(\omega) \times H_0^1(\omega)$.

The presence of the parameter ε^{-2} in front of the bilinear form $\mathscr{A}_S$ in (56) suggests that, when ε is small, a naive discretization (i.e. a standard discretization) will possibly lead to pathologies such as locking phenomenon, which already occurs in considering purely elastic Reissner–Mindlin plates. We thus propose to discretize the bending problem by means of a mixed formulation. More precisely, we here consider an element based on the *linking technique*, presented in Reference [13] and theoretically analysed in Reference [12] within the context of purely elastic plates. We first set

$$\Gamma_h = \left\{ \boldsymbol{s}_h \in L^2(\omega)^2 \colon\ \boldsymbol{s}_{h|K} = (a + b\eta, c + \mathrm{d}\xi)\ \forall K \in \mathscr{T}_h \right\} \tag{57}$$

where (ξ, η) are the standard isoparametric co-ordinates of K.

We then select

$$\Theta_h = \left\{ \boldsymbol{\eta}_h \in H_0^1(\omega)^2 \colon\ \boldsymbol{\eta}_{h|K} \in Q_1(K)^2 \oplus \Gamma_h b_K\ \ \forall K \in \mathscr{T}_h \right\}, \tag{58}$$

where $Q_r(T)$ is the space of polynomials defined on K of degree at most r in each isoparametric co-ordinate ξ and η, while $b_K = (1 - \xi^2)(1 - \eta^2)$. Moreover, we take

$$W_h = \{ \zeta_h \in H_0^1(\omega) \colon\ \zeta_{h|K} \in Q_1(K)\ \forall K \in \mathscr{T}_h \} \tag{59}$$

and

$$\Pi_h = \{ \rho_h \in H_0^1(\omega) \colon\ \rho_{h|K} \in Q_1(K)\ \forall K \in \mathscr{T}_h \} \tag{60}$$

Let us now introduce for each $K \in \mathscr{T}_h$ the functions

$$\varphi_i = \lambda_j \lambda_k \lambda_m \tag{61}$$

In (61) $\{\lambda_i\}_{1 \leqslant i \leqslant 4}$ are the equations of the sides of K and the indices (i, j, k, m) form a permutation of the set $(1, 2, 3, 4)$. Thus, the function φ_i is a sort of edge bubble relatively to the edge e_i of K. Let us set

$$\mathrm{EB}(K) = \mathrm{Span}\{\varphi_i\}_{1 \leqslant i \leqslant 4} \tag{62}$$

We introduce the operator L, which is locally defined (cf. Reference [13]) as

$$L_{|K} \boldsymbol{\eta}_h = \sum_{i=1}^{4} \alpha_i \varphi_i \in \mathrm{EB}(K) \tag{63}$$

by requiring that

$$(\boldsymbol{\eta}_h + \boldsymbol{\nabla} L \boldsymbol{\eta}_h) \cdot \boldsymbol{\tau}_i = \text{constant along each } e_i \tag{64}$$

Therefore, we will deal with the problem

- Find $(\boldsymbol{\theta}_h, w_h, \beta_h; \boldsymbol{\gamma}_h) \in \Theta_h \times W_h \times \Pi_h \times \Gamma_h$, solution of

$$\begin{aligned} a_{\mathscr{B}}(\boldsymbol{\theta}_h, \boldsymbol{\eta}) + (\boldsymbol{\nabla}\beta_h, \boldsymbol{\nabla}\rho) + (\boldsymbol{\gamma}_h, \boldsymbol{\eta} + \boldsymbol{\nabla}(\zeta + L\boldsymbol{\eta}) + \kappa \boldsymbol{\nabla}\rho) &= (\boldsymbol{m}, \boldsymbol{\eta}) + (r, \zeta + L\boldsymbol{\eta}) \\ &\quad + (\psi, \rho) + \kappa(1 + \varepsilon^2)(r, \rho) \\ (\boldsymbol{\theta}_h + \boldsymbol{\nabla}(w_h + L\boldsymbol{\theta}_h) + \kappa \boldsymbol{\nabla}\beta, \boldsymbol{s}) - \varepsilon^2 (\boldsymbol{\gamma}_h, \boldsymbol{s}) &= 0 \end{aligned} \tag{65}$$

for each $(\boldsymbol{\eta}, \zeta, \rho; \boldsymbol{s}) \in \Theta_h \times W_h \times \Pi_h \times \Gamma_h$.

Problem (65) can also be written as

- Find $(\boldsymbol{\theta}_h, w_h, \beta_h; \boldsymbol{\gamma}_h) \in \Theta_h \times W_h \times \Pi_h \times \Gamma_h$, solution of

$$\mathscr{A}_h(\boldsymbol{\theta}_h, w_h, \beta_h, \boldsymbol{\gamma}_h; \boldsymbol{\eta}, \zeta, \rho, \boldsymbol{s}) = \mathscr{L}_{\varepsilon,h}(\boldsymbol{\eta}, \zeta, \rho, \boldsymbol{s}) \quad \forall (\boldsymbol{\eta}, \zeta, \rho; \boldsymbol{s}) \in \Theta_h \times W_h \times \Pi_h \times \Gamma_h \tag{66}$$

where

$$\begin{aligned}\mathscr{A}_h(\boldsymbol{\theta}_h, w_h, \beta_h, \boldsymbol{\gamma}_h; \boldsymbol{\eta}, \zeta, \rho, \boldsymbol{s}) := a_{\mathscr{B}}(\boldsymbol{\theta}_h, \boldsymbol{\eta}) + (\boldsymbol{\nabla}\beta_h, \boldsymbol{\nabla}\rho) + (\boldsymbol{\gamma}_h, \boldsymbol{\eta} + \boldsymbol{\nabla}(\zeta + L\boldsymbol{\eta}) + \kappa\boldsymbol{\nabla}\rho) \\ - (\boldsymbol{\theta}_h + \boldsymbol{\nabla}(w_h + L\boldsymbol{\theta}_h) + \kappa\boldsymbol{\nabla}\beta, \boldsymbol{s}) + \varepsilon^2(\boldsymbol{\gamma}_h, \boldsymbol{s})\end{aligned} \tag{67}$$

and

$$\mathscr{L}_{\varepsilon,h}(\boldsymbol{\eta}, \zeta, \rho, \boldsymbol{s}) : = (\boldsymbol{m}, \boldsymbol{\eta}) + (r, \zeta + L\boldsymbol{\eta}) + (\psi, \rho) + \kappa(1 + \varepsilon^2)(r, \rho) \tag{68}$$

We will develop our stability analysis by means of the norm

$$|||\boldsymbol{\theta}_h, w_h, \beta_h; \boldsymbol{\gamma}_h|||^2 : = ||\boldsymbol{\theta}_h||_1^2 + ||w_h||_1^2 + ||\beta_h||_1^2 + \varepsilon^2||\boldsymbol{\gamma}_h||_0^2 + \sum_{K \in \mathscr{T}_h} h_K^2 ||\boldsymbol{\gamma}_h||_{0,K}^2 \tag{69}$$

We have the following proposition.

Proposition 3.2. Given $(\boldsymbol{\theta}_h, w_h, \beta_h; \boldsymbol{\gamma}_h) \in \Theta_h \times W_h \times \Pi_h \times \Gamma_h$ there exists $(\boldsymbol{\eta}, \zeta, \rho, \boldsymbol{s}) \in \Theta_h \times W_h \times \Pi_h \times \Gamma_h$ such that

$$\mathscr{A}_h(\boldsymbol{\theta}_h, w_h, \beta_h, \boldsymbol{\gamma}_h; \boldsymbol{\eta}, \zeta, \rho, \boldsymbol{s}) \geqslant C|||\boldsymbol{\theta}_h, w_h, \beta_h, \boldsymbol{\gamma}_h|||^2 \tag{70}$$

and

$$|||\boldsymbol{\eta}, \zeta, \rho, \boldsymbol{s}||| \leqslant C|||\boldsymbol{\theta}_h, w_h, \beta_h, \boldsymbol{\gamma}_h||| \tag{71}$$

Proof: Proof We will perform the proof in three steps.

(i) Choose $(\boldsymbol{\eta}_1, \zeta_1, \rho_1, \boldsymbol{s}_1) = (\boldsymbol{\theta}_h, w_h, \beta_h, \boldsymbol{\gamma}_h)$. We easily get

$$\mathscr{A}_h(\boldsymbol{\theta}_h, w_h, \beta_h, \boldsymbol{\gamma}_h; \boldsymbol{\eta}_1, \zeta_1, \rho_1, \boldsymbol{s}_1) \geqslant C(||\boldsymbol{\theta}_h||_1^2 + ||\boldsymbol{\nabla}\beta_h||_1^2 + \varepsilon^2||\boldsymbol{\gamma}_h||_0^2) \tag{72}$$

and

$$|||\boldsymbol{\eta}_1, \zeta_1, \rho_1, \boldsymbol{s}_1||| \leqslant C|||\boldsymbol{\theta}_h, w_h, \beta_h, \boldsymbol{\gamma}_h||| \tag{73}$$

(ii) Choose now $\zeta_2 = 0$, $\rho_2 = 0$, $\boldsymbol{s}_2 = 0$ and $\boldsymbol{\eta}_{2|T} = h_K^2 b_K \boldsymbol{\gamma}_h$. We have, since $L\boldsymbol{\eta}_2 = 0$,

$$\mathscr{A}_h(\boldsymbol{\theta}_h, w_h, \beta_h, \boldsymbol{\gamma}_h; \boldsymbol{\eta}_2, \zeta_2, \rho_2, \boldsymbol{s}_2) = a_{\mathscr{B}}(\boldsymbol{\theta}_h, \boldsymbol{\eta}_2) + \sum_{K \in \mathscr{T}_h} h_K^2 (\boldsymbol{\gamma}_h, b_K \boldsymbol{\gamma}_h)_K \tag{74}$$

which easily implies

$$\mathscr{A}_h(\boldsymbol{\theta}_h, w_h, \beta_h, \boldsymbol{\gamma}_h; \boldsymbol{\eta}_2, \zeta_2, \rho_2, \boldsymbol{s}_2) \geqslant a_{\mathscr{B}}(\boldsymbol{\theta}_h, \boldsymbol{\eta}_2) + C \sum_{K \in \mathscr{T}_h} h_K^2 ||\boldsymbol{\gamma}_h||_{0,K}^2 \tag{75}$$

Moreover,

$$a_{\mathscr{B}}(\boldsymbol{\theta}_h, \boldsymbol{\eta}_2) \geqslant -\frac{M}{2\delta}||\boldsymbol{\theta}_h||_1^2 - \frac{M\delta}{2}||\boldsymbol{\eta}_2||_1^2 \geqslant -\frac{M}{2\delta}||\boldsymbol{\theta}_h||_1^2 - \frac{C\delta}{2}\sum_{K \in \mathscr{T}_h} h_K^2 ||\boldsymbol{\gamma}_h||_{0,K}^2 \tag{76}$$

for $\delta > 0$. Taking δ sufficiently small, we get

$$\mathscr{A}_h(\boldsymbol{\theta}_h, w_h, \beta_h, \boldsymbol{\gamma}_h; \boldsymbol{\eta}_2, \zeta_2, \rho_2, \boldsymbol{s}_2) \geqslant C_2 \sum_{K \in \mathscr{T}_h} h_K^2 ||\boldsymbol{\gamma}_h||_{0,K}^2 - C_3 ||\boldsymbol{\theta}_h||_1^2 \tag{77}$$

Finally, an easy scaling argument shows that it holds

$$|||\boldsymbol{\eta}_2, \zeta_2, \rho_2, \boldsymbol{s}_2||| \leqslant C |||\boldsymbol{\theta}_h, w_h, \beta_h, \boldsymbol{\gamma}_h||| \tag{78}$$

(iii) It remains to get control on the deflections. To this end, we select $\boldsymbol{\eta}_3 = 0$, $\zeta_3 = 0$, $\rho_3 = 0$ and $\boldsymbol{s}_3 = -\boldsymbol{\nabla} w_h$. We thus get

$$\mathscr{A}_h(\boldsymbol{\theta}_h, w_h, \beta_h, \boldsymbol{\gamma}_h; \boldsymbol{\eta}_3, \zeta_3, \rho_3, \boldsymbol{s}_3) = ||\boldsymbol{\nabla} w_h||_0^2 + (\boldsymbol{\theta}_h + \boldsymbol{\nabla} L \boldsymbol{\theta}_h, \boldsymbol{\nabla} w_h) + (\kappa \boldsymbol{\nabla} \beta, \boldsymbol{\nabla} w_h) + \varepsilon^2 (\boldsymbol{\gamma}_h, \boldsymbol{\nabla} w_h) \tag{79}$$

Using the technique in (ii) we may obtain

$$\mathscr{A}_h(\boldsymbol{\theta}_h, w_h, \beta_h, \boldsymbol{\gamma}_h; \boldsymbol{\eta}_3, \zeta_3, \rho_3, \boldsymbol{s}_3) \geqslant C_4 ||\boldsymbol{\nabla} w_h||_0^2 - C_5 ||\boldsymbol{\theta}_h||_1^2 - C_6 ||\boldsymbol{\nabla} \beta||_0^2 - C_7 \varepsilon^2 ||\boldsymbol{\gamma}_h||_0^2 \tag{80}$$

Furthermore we have

$$|||\boldsymbol{\eta}_3, \zeta_3, \rho_3, \boldsymbol{s}_3||| \leqslant C |||\boldsymbol{\theta}_h, w_h, \beta_h, \boldsymbol{\gamma}_h||| \tag{81}$$

Now, taking a suitable linear combination of $\{(\boldsymbol{\eta}_i, \zeta_i, \rho_i, \boldsymbol{s}_i)\}_{i=1}^3$ gives the result. The proof is then complete. □

In the error analysis which follows, we will use a result concerning the linking operator L, whose proof can be found in Reference [12]. In fact, we have

Lemma 3.1. Let $(\cdot)_{\mathrm{I}}$ denote the usual Lagrange interpolating operator over the piecewise bilinear and continuous functions, and $(\cdot)_{\mathrm{II}}$ denote the Lagrange interpolating operator over the piecewise bilinear and continuous vectorial functions. Then we have

$$|\zeta - \zeta_{\mathrm{I}} + L((\boldsymbol{\nabla})_{\mathrm{II}})|_1 \leqslant C h^2 |\zeta|_3 \quad \forall \zeta \in H^3(\omega) \tag{82}$$

and

$$|L \boldsymbol{\eta}_h|_1 \leqslant C h |\boldsymbol{\eta}_h|_1 \quad \forall \boldsymbol{\eta}_h \in \Theta_h \tag{83}$$

By using the techniques developed in Reference [12], it is not hard to obtain the following error estimate.

Proposition 3.3. Let $(\boldsymbol{\theta}_h, w_h, \beta_h, \boldsymbol{\gamma}_h) \in \Theta_h \times W_h \times \Pi_h \times \Gamma_h$ be the solution of the discretized problem (65); let $(\boldsymbol{\theta}, w, \beta, \boldsymbol{\gamma}) \in H_0^1(\omega)^2 \times H_0^1(\omega) \times H_0^1(\omega) \times L^2(\omega)^2$ be the solution of the continuous problem (45). Then we have

$$||\boldsymbol{\theta}_h - \boldsymbol{\theta}||_1 + ||w_h - w||_1 + ||\beta_h - \beta||_1 + \left(\sum_{K \in \mathscr{T}_h} h_K^2 ||\boldsymbol{\gamma}_h - \boldsymbol{\gamma}||_{0,K}^2 \right)^{1/2} + \varepsilon ||\boldsymbol{\gamma}_h - \boldsymbol{\gamma}||_0 \leqslant C h \tag{84}$$

Proof: We only sketch the proof, since it is very similar to that given in Reference [12]. Let $\boldsymbol{\theta}_{\mathrm{II}} \in \Theta_h$ be the Lagrange interpolant of $\boldsymbol{\theta}$; $w_{\mathrm{I}} \in W_h$ and $\beta_{\mathrm{I}} \in \Pi_h$ be the ones for w and β, respectively. Finally, let $\boldsymbol{\gamma}^* \in \Gamma_h$ be the $L^2(\omega)$-projection of $\boldsymbol{\gamma}$. By Proposition 3.2, there exists $(\boldsymbol{\eta}, \zeta, \rho, \boldsymbol{s}) \in \Theta_h \times W_h \times \Pi_h \times \Gamma_h$ such that

$$C |||\boldsymbol{\theta}_h - \boldsymbol{\theta}_{\mathrm{II}}, w_h - w_{\mathrm{I}}, \beta_h - \beta_{\mathrm{I}}, \boldsymbol{\gamma}_h - \boldsymbol{\gamma}^*|||^2 \leqslant \mathscr{A}_h(\boldsymbol{\theta}_h - \boldsymbol{\theta}_{\mathrm{II}}, w_h - w_{\mathrm{I}}, \beta_h - \beta_{\mathrm{I}}, \boldsymbol{\gamma}_h - \boldsymbol{\gamma}^*; \boldsymbol{\eta}, \zeta, \rho, \boldsymbol{s}) \tag{85}$$

and

$$|||\boldsymbol{\eta}, \zeta, \rho, \boldsymbol{s}||| \leqslant C|||\boldsymbol{\theta}_h - \boldsymbol{\theta}_{\mathrm{II}}, w_h - w_{\mathrm{I}}, \beta_h - \beta_{\mathrm{I}}, \boldsymbol{\gamma}_h - \boldsymbol{\gamma}^*||| \tag{86}$$

Hence, we have

$$\begin{aligned} C|||\boldsymbol{\theta}_h - \boldsymbol{\theta}_{\mathrm{II}}, w_h - w_{\mathrm{I}}, \beta_h - \beta_{\mathrm{I}}, \boldsymbol{\gamma}_h - \boldsymbol{\gamma}^*|||^2 \leqslant a_{\mathscr{B}}(\boldsymbol{\theta} - \boldsymbol{\theta}_{\mathrm{II}}, \boldsymbol{\eta}) + (\boldsymbol{\nabla}(\beta - \beta_{\mathrm{I}}), \boldsymbol{\nabla}\rho) + (\boldsymbol{\gamma} - \boldsymbol{\gamma}^*, \boldsymbol{\eta} \\ + \boldsymbol{\nabla}(\zeta + L\boldsymbol{\eta}) + \kappa\boldsymbol{\nabla}\rho) - (\boldsymbol{\theta} - \boldsymbol{\theta}_{\mathrm{II}} + \boldsymbol{\nabla}[(w + \kappa\beta) - (w + \kappa\beta)_{\mathrm{I}}] - \boldsymbol{\nabla}L\boldsymbol{\theta}_{\mathrm{II}}, \boldsymbol{s}) + \varepsilon^2(\boldsymbol{\gamma} - \boldsymbol{\gamma}^*, \boldsymbol{s}) \end{aligned} \tag{87}$$

Above, the only term which is not straightforward to bound is

$$(\boldsymbol{\nabla}[(w + \kappa\beta) - (w + \kappa\beta)_{\mathrm{I}}] - \boldsymbol{\nabla}L\boldsymbol{\theta}_{\mathrm{II}}, \boldsymbol{s}) \tag{88}$$

We notice that

$$\varepsilon^2\boldsymbol{\gamma} = \boldsymbol{\theta} + \boldsymbol{\nabla}(w + \kappa\beta) \tag{89}$$

so that

$$\boldsymbol{\theta}_{\mathrm{II}} = \varepsilon^2\boldsymbol{\gamma}_{\mathrm{II}} - [\boldsymbol{\nabla}(w + \kappa\beta)]_{\mathrm{II}} \tag{90}$$

Hence, our term to treat turns out to be

$$(\boldsymbol{\nabla}[(w + \kappa\beta) - (w + \kappa\beta)_{\mathrm{I}}] + \boldsymbol{\nabla}L[\boldsymbol{\nabla}(w + \kappa\beta)]_{\mathrm{II}}, \boldsymbol{s}) + \varepsilon^2(\boldsymbol{\nabla}L\boldsymbol{\gamma}_{\mathrm{II}}, \boldsymbol{s}) \tag{91}$$

By using Lemma 3.1 we easily get

$$\begin{aligned} &(\boldsymbol{\nabla}[(w + \kappa\beta) - (w + \kappa\beta)_{\mathrm{I}}] + \boldsymbol{\nabla}L[\boldsymbol{\nabla}(w + \kappa\beta)]_{\mathrm{II}}, \boldsymbol{s}) + \varepsilon^2(\boldsymbol{\nabla}L\boldsymbol{\gamma}_{\mathrm{II}}, \boldsymbol{s}) \\ &\quad \leqslant Ch\left(\left(\sum_{K \in \mathscr{T}_h} h_K^2 ||\boldsymbol{s}||_{0,K}^2\right)^{1/2} + \varepsilon||\boldsymbol{s}||_0\right) \end{aligned} \tag{92}$$

From (87) we obtain

$$|||\boldsymbol{\theta}_h - \boldsymbol{\theta}_{\mathrm{II}}, w_h - w_{\mathrm{I}}, \beta_h - \beta_{\mathrm{I}}, \boldsymbol{\gamma}_h - \boldsymbol{\gamma}^*|||^2 \leqslant Ch|||\boldsymbol{\theta}_h - \boldsymbol{\theta}_{\mathrm{II}}, w_h - w_{\mathrm{I}}, \beta_h - \beta_{\mathrm{I}}, \boldsymbol{\gamma}_h - \boldsymbol{\gamma}^*||| \cdot |||\boldsymbol{\eta}, \zeta, \rho, \boldsymbol{s}||| \tag{93}$$

by which, using (86) and the triangle inequality, we get (84).

4. NUMERICAL TESTS

Aim of this section is to present some numerical tests showing the behaviour of the interpolating schemes previously considered, relevant to both membranal and bending problems. The schemes have been implemented into the finite element analysis program (FEAP) (cf. Reference [16]), and their performances have been checked on a series of model problems for which the analytical solutions can be easily obtained. This allows to determine the discrete-solution error.

Table I. Piezoelectric ceramic PZT-5H. Elastic, dielectric and piezoelectric properties.

c_{11} (GPa)	126
c_{12} (GPa)	79.5
c_{13} (GPa)	84.1
c_{33} (GPa)	117
c_{44} (GPa)	23.0
ε_{11} (nF/m)	15.0
ε_{33} (nF/m)	13.0
e_{31} (C/m^2)	−6.5
e_{33} (C/m^2)	23.3
e_{15} (C/m^2)	17.0

The model problems consider a square plate of unit side. Two different aspect ratios are investigated: $t/l = 0.001$ and 0.2, corresponding to a 'thin' and a 'thick' plate, respectively. The plate is simply supported and grounded along its boundary, and is comprised by a homogeneous linearly piezoelectric transversely isotropic material, whose elastic, dielectric and piezoelectric properties are reported in Table I. The in-plane characteristic length l is taken equal to the side of the plate. The Cartesian frame is chosen such that the middle cross-section is $\omega = [0,1] \times [0,1]$.

All the analyses are performed using regular meshes and discretizing only one-quarter of the plate, due to symmetry considerations.

4.1. Membranal problems

The following three loading conditions are considered:

- Load a:

$$\boldsymbol{r} = r_0 \begin{bmatrix} \cos(\pi y_1)\sin(\pi y_2) \\ \sin(\pi y_1)\cos(\pi y_2) \end{bmatrix}$$
$$\upsilon = 0$$

- Load b:

$$\boldsymbol{r} = r_0 \begin{bmatrix} \cos(\pi y_1)\sin(\pi y_2) \\ -\sin(\pi y_1)\cos(\pi y_2) \end{bmatrix}$$
$$\upsilon = 0$$

- Load c:

$$\boldsymbol{r} = \boldsymbol{0}$$
$$\upsilon = \upsilon_0 \sin(\pi y_1)\sin(\pi y_2)$$

Under the previous loading conditions, the analytical solutions of system (10) are, respectively, given by

- Load a:

$$\boldsymbol{u} = \frac{r_0(1+2\delta^2\pi^2)}{2\pi^2(1+\xi^2+2\delta^2\pi^2)} \begin{bmatrix} \cos(\pi y_1)\sin(\pi y_2) \\ \sin(\pi y_1)\cos(\pi y_2) \end{bmatrix}$$

$$\chi = -\frac{\xi r_0}{\pi(1+\xi^2+2\delta^2\pi^2)} \sin(\pi y_1)\sin(\pi y_2)$$

- Load b:

$$\boldsymbol{u} = \frac{r_0}{\pi^2(1-\nu)} \begin{bmatrix} \cos(\pi y_1)\sin(\pi y_2) \\ -\sin(\pi y_1)\cos(\pi y_2) \end{bmatrix}$$

$$\chi = 0$$

- Load c:

$$\boldsymbol{u} = \frac{\xi \upsilon_0}{2\pi(1+\xi^2+2\delta^2\pi^2)} \begin{bmatrix} \cos(\pi y_1)\sin(\pi y_2) \\ \sin(\pi y_1)\cos(\pi y_2) \end{bmatrix}$$

$$\chi = \frac{\upsilon_0}{1+\xi^2+2\delta^2\pi^2} \sin(\pi y_1)\sin(\pi y_2)$$

The results obtained in the numerical computations are reported, respectively, in Tables II–IV together with the analytical solutions. In the tables, the unknown u_2 is computed at the point $P_2(1/2, 0)$, while the unknown χ is computed at $P_1(1/2, 1/2)$.

The error of a discrete solution is measured as

$$E_f^2 = \frac{\sum_{N_i}(f_h(N_i) - f(N_i))^2}{\sum_{N_i} f(N_i)^2} \tag{94}$$

where the field f is either u_1, u_2 or χ and the sum is performed over all the nodal points N_i. It is pointed out that the above error measure can be seen as discrete L^2-type error.

Figures 1 and 2 show the relative errors versus the number of nodes per side, respectively, for the case of thin and thick plate. Load cases a, b and c are plotted by using solid, dotted and dash–dot lines, respectively. The error lines for the fields u_2 and χ are distinguished by using a circle and a $\times$-mark, respectively. It is interesting to observe that both the figures show the quadratic convergence rate for all the unknown fields and all the loading conditions. Of course, the attained h^2 convergence rate in these norm actually means a h^1 convergence rate in the H^1 energy-type norm.

4.2. *Bending problems*

The following four loading conditions are considered:

- Load a:

$$r = r_0 \sin(\pi y_1)\sin(\pi y_2)$$

$$\boldsymbol{m} = \boldsymbol{0}$$

$$\psi = 0$$

Table II. Membranal problem. Load case *a*. $r_0 = 1$. Numerical and analytical solutions for thin and thick plates.

	Thin		Thick	
Mesh	$100u_2(P_2)$	$10\chi(P_1)$	$100u_2(P_2)$	$10\chi(P_1)$
2×2	3.7422	1.6039	3.8591	1.4925
4×4	3.5216	1.5126	3.6300	1.4121
8×8	3.4695	1.4904	3.5758	1.3924
16×16	3.4566	1.4849	3.5625	1.3875
32×32	3.4534	1.4835	3.5591	1.3863
64×64	3.4526	1.4831	3.5583	1.3860
Analytical	3.4524	1.4830	3.5580	1.3859

Table III. Membranal problem. Load case *a*. $r_0 = 1$. Numerical and analytical solutions for thin and thick plates.

	Thin		Thick	
Mesh	$10u_2(P_2)$	$\chi(P_1)$	$10u_2(P_2)$	$\chi(P_1)$
2×2	−1.4326	0	−1.4326	0
4×4	−1.4298	0	−1.4298	0
8×8	−1.4287	0	−1.4287	0
16×16	−1.4284	0	−1.4284	0
32×32	−1.4283	0	−1.4283	0
64×64	−1.4283	0	−1.4283	0
Analytical	−1.4283	0	−1.4283	0

Table IV. Membranal problem. Load case *c*. $v_0 = 1$. Numerical and analytical solutions for thin and thick plates.

	Thin		Thick	
Mesh	$10^2u_2(P_2)$	$10\chi(P_1)$	$10^2u_2(P_2)$	$10\chi(P_1)$
2×2	−8.0194	7.6383	−7.4625	7.1076
4×4	−7.5629	7.0115	−7.0604	6.5457
8×8	−7.4519	6.8632	−6.9621	6.3792
16×16	−7.4243	6.8269	−6.9377	6.3792
32×32	−7.4174	6.8176	−6.9316	6.3709
64×64	−7.4157	6.8155	−6.9301	6.3694
Analytical	−7.4151	6.8146	−6.9296	6.3684

- Load *b*:

$$r = 0$$
$$\boldsymbol{m} = m_0 \begin{bmatrix} \cos(\pi y_1)\sin(\pi y_2) \\ \sin(\pi y_1)\cos(\pi y_2) \end{bmatrix}$$
$$\psi = 0$$

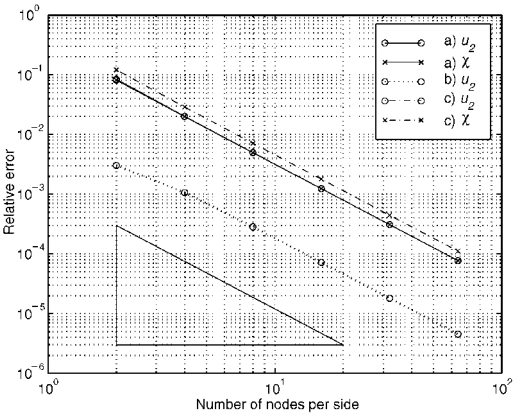

Figure 1. Membranal solutions for a thin-plate problem. Load cases a, b and c. Relative error for the unknown fields u_2 and χ versus number of nodes per side. The attainment of the h^2 convergence rate in the L^2 error norm clearly appears.

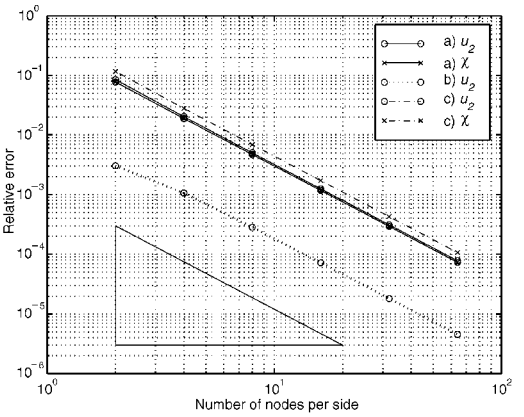

Figure 2. Membranal solutions for a thick-plate problem. Load cases a, b and c. Relative error for the unknown fields u_2 and χ versus number of nodes per side. The attainment of the h^2 convergence rate in the L^2 error norm clearly appears.

- Load c:

$$\begin{aligned} r &= 0 \\ \boldsymbol{m} &= m_0 \begin{bmatrix} \cos(\pi y_1)\sin(\pi y_2) \\ -\sin(\pi y_1)\cos(\pi y_2) \end{bmatrix} \\ \psi &= 0 \end{aligned}$$

- Load d:

$$\begin{aligned} r &= 0 \\ \boldsymbol{m} &= \mathbf{0} \\ \psi &= \psi_0 \sin(\pi y_1)\sin(\pi y_2) \end{aligned}$$

Under the previous loading conditions, the analytical solutions of system (26) are, respectively, given by

- Load a:

$$\begin{aligned} \boldsymbol{\theta} &= -\frac{r_0}{4\pi^3} \begin{bmatrix} \cos(\pi y_1)\sin(\pi y_2) \\ \sin(\pi y_1)\cos(\pi y_2) \end{bmatrix} \\ w &= \frac{r_0}{4\pi^4}[1 + 2\pi^2\varepsilon^2(1-\kappa^2)]\sin(\pi y_1)\sin(\pi y_2) \\ \beta &= \frac{\kappa r_0}{2\pi^2}\varepsilon^2 \sin(\pi y_1)\sin(\pi y_2) \end{aligned}$$

Table V. Bending problem. Load case *a*. $r_0 = 1$. Numerical and analytical solutions for thin and thick plates.

Mesh	Thin			Thick		
	$10^3\theta_2(P_2)$	$10^3 w(P_1)$	$10^8\beta(P_1)$	$10^3\theta_2(P_2)$	$10^3 w(P_1)$	$10^4\beta(P_1)$
2×2	−8.4852	2.5393	1.2545	−8.5281	2.9497	5.0179
4×4	−8.1722	2.5623	1.2074	−8.1747	2.9519	4.8297
8×8	−8.0904	2.5656	1.1960	−8.0906	2.9512	4.7834
16×16	−8.0698	2.5663	1.1930	−8.0698	2.9509	4.7719
32×32	−8.0646	2.5665	1.1922	−8.0646	2.9508	4.7691
64×64	−8.0633	2.5665	1.1920	−8.0633	2.9508	4.7683
Analytical	−8.0629	2.5665	1.1920	−8.0629	2.9508	4.7681

- Load *b*:

$$\boldsymbol{\theta} = \frac{m_0}{2\pi^2}\begin{bmatrix}\cos(\pi y_1)\sin(\pi y_2)\\ \sin(\pi y_1)\cos(\pi y_2)\end{bmatrix}$$
$$w = -\frac{m_0}{2\pi^3}\sin(\pi y_1)\sin(\pi y_2)$$
$$\beta = 0$$

- Load *c*:

$$\boldsymbol{\theta} = \frac{m_0\varepsilon^2}{1+\pi^2\varepsilon^2(1-\mu)}\begin{bmatrix}\cos(\pi y_1)\sin(\pi y_2)\\ -\sin(\pi y_1)\cos(\pi y_2)\end{bmatrix}$$
$$w = 0$$
$$\beta = 0$$

- Load *d*:

$$\boldsymbol{\theta} = \mathbf{0}$$
$$w = -\frac{\kappa\psi_0}{2\pi^2}\sin(\pi y_1)\sin(\pi y_2)$$
$$\beta = \frac{\psi_0}{2\pi^2}\sin(\pi y_1)\sin(\pi y_2)$$

The results obtained in the numerical computations are reported, respectively, in Tables V–VIII together with the analytical solutions. In the tables, the unknowns w and β are computed at the point $P_1(\frac{1}{2}, \frac{1}{2})$, while the unknown θ_2 is computed at $P_2(\frac{1}{2}, 0)$.

The error of a discrete solution is measured as indicated in Equation (94), where f is either w, θ_1, θ_2 or β. For simplicity, the summations are performed on all the nodes N_i relative to global interpolation parameters (that is, in the error evaluation the internal parameters associated with bubble functions are neglected).

Figures 3 and 4 show the relative errors versus the number of nodes per side, respectively, for the case of thin and thick plate. Load cases *a*, *b*, *c* and *d* are plotted by using solid, dotted, dash–dot and dashed lines, respectively. The error lines for the fields w, θ_2 and β are distinguished by using a circle, a $\times$-mark and a square, respectively.

Table VI. Bending problem. Load case *b*. $m_0 = 1$. Numerical and analytical solutions for thin and thick plates.

Mesh	Thin			Thick		
	$10^2\theta_2(P_2)$	$10^2 w(P_1)$	$\beta(P_1)$	$10^2\theta_2(P_2)$	$10^2 w(P_1)$	$\beta(P_1)$
2×2	5.3262	−1.5963	0	5.3516	−1.5998	0
4×4	5.1344	−1.6099	0	5.1360	−1.6102	0
8×8	5.0833	−1.6120	0	5.0834	−1.6120	0
16×16	5.0704	−1.6124	0	5.0704	−1.6124	0
32×32	5.0672	−1.6125	0	5.0672	−1.6125	0
64×64	5.0663	−1.6126	0	5.0663	−1.6126	0
Analytical	5.0661	−1.6126	0	5.0661	−1.6126	0

Table VII. Bending problem. Load case *c*. $m_0 = 1$. Numerical and analytical solutions for thin and thick plates.

Mesh	Thin			Thick		
	$10^7\theta_2(P_2)$	$w(P_1)$	$\beta(P_1)$	$10^2\theta_2(P_2)$	$w(P_1)$	$\beta(P_1)$
2×2	679.61	0	0	−1.3167	0	0
4×4	40.843	0	0	−1.3102	0	0
8×8	−0.68873	0	0	−1.3079	0	0
16×16	−3.3102	0	0	−1.3073	0	0
32×32	−3.4742	0	0	−1.3071	0	0
64×64	−3.4844	0	0	−1.3071	0	0
Analytical	−3.4851	0	0	−1.3071	0	0

Table VIII. Bending problem. Load case *d*. $\psi_0 = 1$. Numerical and analytical solutions for thin and thick plates.

Mesh	Thin			Thick		
	$\theta_2(P_2)$	$10^2 w(P_1)$	$10^2\beta(P_1)$	$\theta_2(P_2)$	$10^2 w(P_1)$	$10^2\beta(P_1)$
2×2	0	−3.5996	5.3315	0	−3.5996	5.3315
4×4	0	−3.4646	5.1314	0	−3.4646	5.1314
8×8	0	−3.4314	5.0824	0	−3.4314	5.0824
16×16	0	−3.4231	5.0701	0	−3.4231	5.0701
32×32	0	−3.4211	5.0671	0	−3.4211	5.0671
64×64	0	−3.4206	5.0663	0	−3.4206	5.0663
Analytical	0	−3.4204	5.0661	0	-3.4204	5.0661

It is worth noting that:

- at least the quadratic convergence rate for all the unknown fields and all the loading conditions is attained; as said above, the attained h^2 convergence rate in these norm actually means a h^1 convergence rate in the H^1 energy-type norm.

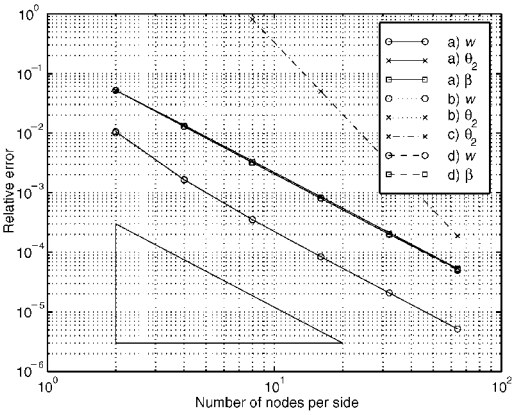

Figure 3. Bending solutions for a thin-plate problem. Load cases a, b, c and d. Relative error for the unknown fields w, θ_2 and β versus number of nodes per side. The attainment of the h^2 convergence rate in the L^2 error norm clearly appears.

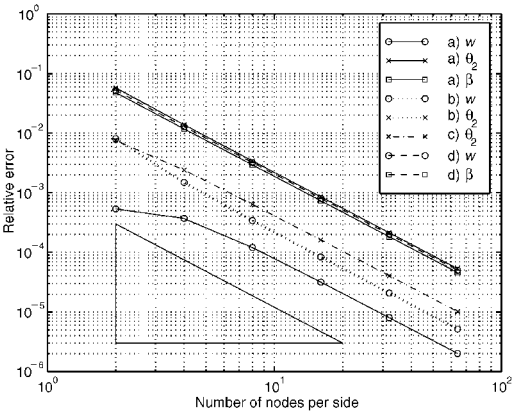

Figure 4. Bending solutions for a thick-plate problem. Load cases a, b, c and d. Relative error for the unknown fields w, θ_2 and β versus number of nodes per side. The attainment of the h^2 convergence rate in the L^2 error norm clearly appears.

- the presented method is fully insensitive to the variation of thickness, in such a way that the error graphics for different choices of the aspect ratio all show at least a quadratic convergence rate. As a consequence, the proposed element is actually locking-free and it can be used for both thin and thick piezoelectric plate problems.

5. CONCLUSIONS

The numerical schemes proposed have been tested on a series of model problems; the numerical investigations clearly show that the adopted schemes have the appropriate convergence rate.

In conclusion, the present study highlights that the only possible pathology associated with a finite-element discretization based on the piezoelectric plate model proposed in Reference [10] is the classical locking phenomenon. At the same time, both the theoretical and the numerical investigations show that a typical locking treatment as proposed in Reference [12] is sufficient to overcome the same effect for the piezoelectric case.

Finally, we observe that if very special situations would occur advising the use of higher-order theories of piezoelectric plates, then numerical treatments of those theories would be required. To the authors' knowledge, such treatments are not available in the literature. The present work can constitute a guide for the theoretical development and evaluation of numerical treatments of high-order theories.

APPENDIX A: AN ABSTRACT CONVERGENCE RESULT

The aim of this section is to slightly extend the convergence result given in Reference [17]. More precisely, the following variational problem is studied:

- Find $u_\varepsilon \in V$, solution of

$$a_\varepsilon(u_\varepsilon, v) := a_0(u_\varepsilon, v) + \varepsilon^{-2} a_1(u_\varepsilon, v) = L_\varepsilon(v) \quad \forall v \in V \tag{A1}$$

Above, V is a Hilbert space with norm $||\cdot||$, $a_0(\cdot,\cdot)$ and $a_1(\cdot,\cdot)$ are continuous symmetric positive-semidefinite bilinear forms, and L_ε belongs to V', the topological dual space of V. Moreover, ε is a real parameter such that $0 < \varepsilon \leqslant \varepsilon_0$. We are interested in studying the behaviour of the solution u_ε as $\varepsilon \to 0$, under suitable hypotheses generally met in most applications, especially in the linear theory of thin structures. We remark that such an analysis has been already developed in Reference [17] for the case of $L_\varepsilon \in V'$ independent of ε. We make the following assumptions:

- The form $a_0(\cdot,\cdot) + a_1(\cdot,\cdot)$ is coercive on V, i.e. there exists $\alpha > 0$ such that

$$a_0(v, v) + a_1(v, v) \geqslant \alpha ||v||^2 \quad \forall v \in V \tag{A2}$$

- The kernel K of $a_1(\cdot,\cdot)$, defined by

$$K := \{v \in V : \ a_1(v, v) = 0\} \tag{A3}$$

  is not trivial, i.e. $K \neq (0)$.
- L_ε strongly converges in V' to a functional $L_0 \in V'$, as $\varepsilon \to 0$.

We are now ready to prove the following.

Proposition A.1. Under the above hypotheses, problem (A1) has a unique solution $u_\varepsilon \in V$. Furthermore, u_ε strongly converges in V, as $\varepsilon \to 0$, to $u_0 \in K$, solution of the variational problem

- Find $u_0 \in K$, such that

$$a_0(u_0, v_0) = L_0(v_0) \quad \forall v_0 \in K \tag{A4}$$

Finally, $u_0 = 0$ if and only if $L_0 \in K^0$, K^0 being the polar set of K.

Proof: The proof follows the guidelines detailed in Reference [17]. First of all, by Lax–Milgram lemma (cf. also (A2)) one has that problem (A7) is uniquely solvable. Choosing in (A1) $v = u_\varepsilon$ one obtains

$$\alpha ||u_\varepsilon||^2 \leqslant a_\varepsilon(u_\varepsilon, u_\varepsilon) = L_\varepsilon(u_\varepsilon) \leqslant C||u_\varepsilon|| \tag{A5}$$

where the last inequality follows also from the strong convergence hypothesis $L_\varepsilon \to L_0$. Hence we have that the family (u_ε) is bounded in V. Therefore, there exists a subsequence of (u_ε), still denoted by (u_ε), which weakly converges to a certain limit $w_0 \in V$. We now multiply Equation (A1) by ε^2, thus obtaining

$$\varepsilon^2 a_0(u_\varepsilon, v) + a_1(u_\varepsilon, v) = \varepsilon^2 L_\varepsilon(v) \quad \forall v \in V \tag{A6}$$

Passing to the limit as $\varepsilon \to 0$, since $u_\varepsilon \to w_0$ weakly, and since the dual norms $||L_\varepsilon||_*$ are bounded uniformly in ε, one has

$$a_1(w_0, v) = 0 \quad \forall v \in V \tag{A7}$$

Hence $w_0 \in K$. Next, we choose $v \in K$ in Equation (A1) and find that

$$a_0(u_\varepsilon, v) = L_\varepsilon(v) \quad \forall v \in K \tag{A8}$$

Again, passing to the limit as $\varepsilon \to 0$, one has that the limit w_0 solves

$$a_0(w_0, v) = L_0(v) \quad \forall v \in K \tag{A9}$$

Since, by Lax–Milgram lemma, the variational problem (A4) has a unique solution $u_0 \in K$, it follows that $w_0 = u_0$. We proceed by showing that the convergence of the subsequence (u_ε) to u_0 is indeed strong. We have

$$\alpha ||u_\varepsilon - u_0||^2 \leqslant a_\varepsilon(u_\varepsilon - u_0, u_\varepsilon - u_0) = a_\varepsilon(u_\varepsilon, u_\varepsilon) - 2a_\varepsilon(u_\varepsilon, u_0) + a_\varepsilon(u_0, u_0) \tag{A10}$$

As we have

$$a_\varepsilon(u_0, u_0) = a_0(u_0, u_0) = L_0(u_0) \tag{A11}$$

and

$$a_\varepsilon(u_\varepsilon, u_\varepsilon) = L_\varepsilon(u_\varepsilon) \tag{A12}$$

and

$$a_\varepsilon(u_\varepsilon, u_0) = L_\varepsilon(u_0) \tag{A13}$$

from (A10) we get

$$\alpha ||u_\varepsilon - u_0||^2 \leqslant (L_\varepsilon(u_\varepsilon) - L_\varepsilon(u_0)) + (L_0 - L_\varepsilon)(u_0) \tag{A14}$$

Since

$$\lim_{\varepsilon \to 0} L_\varepsilon(u_\varepsilon) = L_0(u_0) \tag{A15}$$

and

$$\lim_{\varepsilon \to 0} L_\varepsilon(u_0) = L_0(u_0) \tag{A16}$$

and

$$\lim_{\varepsilon \to 0} (L_0 - L_\varepsilon)(u_0) = 0 \tag{A17}$$

it follows from (A14) that

$$\lim_{\varepsilon \to 0} ||u_\varepsilon - u_0||^2 = 0 \tag{A18}$$

Hence $u_\varepsilon \to u_0$ strongly in V. To summarize, we have shown that any weakly convergent subsequence of (u_ε) converges indeed *strongly* to the same limit $u_0 \in K$, solution of problem (A4). This means that the only cluster point of the whole family (u_ε) is u_0. As (u_ε) is bounded, it follows that the whole family strongly converges to u_0. The proof is thus complete. □

APPENDIX B: A BRIEF DERIVATION OF THE PIEZOELECTRIC PLATE MODEL

In this section we outline a brief derivation of the piezoelectric plate model proposed in Reference [6], in order to emphasize the hypotheses on which this model is based. For a more detailed discussion, we refer to the original paper.

As a starting point, we consider a weak formulation [4] of the Voigt theory of piezoelectricity. It is a generalization to piezoelectric bodies of the classical Hellinger–Prange–Reissner functional

of linear elasticity

$$\begin{aligned}\mathscr{H} = \frac{1}{2}\int_A [&-(s_{11}-s_{12})||\mathbf{T}||^2 - s_{12}(\operatorname{tr}\mathbf{T})^2 - s_{33}\sigma^2 + \beta_{33}d^2 - 2s_{13}\sigma(\operatorname{tr}\mathbf{T})\\ &-2g_{31}d(\operatorname{tr}\mathbf{T}) - 2g_{33}\sigma d - s_{44}||\boldsymbol{\tau}||^2 + \beta_{11}||\boldsymbol{d}||^2 - 2g_{15}\boldsymbol{\tau}\cdot\boldsymbol{d}]\,\mathrm{d}v\\ &+\int_A [\mathbf{T}\cdot\boldsymbol{\nabla}^S\boldsymbol{S} + \boldsymbol{\tau}\cdot(\boldsymbol{S}' + \boldsymbol{\nabla}S) + \sigma S' + \boldsymbol{d}\cdot\boldsymbol{\nabla}\Phi + d\Phi']\,\mathrm{d}v\\ &-\int_\Omega [\boldsymbol{P}^{\pm}\cdot\boldsymbol{S}(\cdot,\pm t/2) + P^{\pm}S(\cdot,\pm t/2) - \Upsilon^{\pm}\Phi(\cdot,\pm t/2)]\,\mathrm{d}a\\ &-\int_{\partial\Omega\times(-t/2,t/2)} [\mathbf{T}\boldsymbol{n}\cdot\boldsymbol{S} + (\boldsymbol{\tau}\cdot\boldsymbol{n})S + (\boldsymbol{d}\cdot\boldsymbol{n})\Phi]\,\mathrm{d}a \end{aligned} \tag{B1}$$

Here $\mathbf{T}$ is the in-plane stress, $\boldsymbol{\tau}$ is the transversal shear stress, σ is the normal stress in the thickness direction, $\boldsymbol{d}$ is the in-plane electric displacement, d is the electric displacement in the thickness direction, tr denotes the trace operator, an apex denotes the differentiation with respect to ζ and $\boldsymbol{n}$ is the exterior normal to the lateral boundary of the plate. The material constants s_{11}, s_{33}, s_{44}, s_{12} and s_{13} are the 'open-circuit' elastic compliances; β_{11} and β_{33} are the 'free' impermeability constants; g_{31}, g_{33} and g_{15} are the 'open-circuit/free' piezoelectric constants. They are related to the material constants introduced in Section 2 by the equations [1]:

$$\begin{bmatrix} s_{11} & s_{12} & s_{13} & g_{31}\\ s_{12} & s_{11} & s_{13} & g_{31}\\ s_{13} & s_{13} & s_{33} & g_{33}\\ -g_{31} & -g_{31} & -g_{33} & \beta_{33}\end{bmatrix} = \begin{bmatrix} c_{11} & c_{12} & c_{13} & -e_{31}\\ c_{12} & c_{11} & c_{13} & -e_{31}\\ c_{13} & c_{13} & c_{33} & -e_{33}\\ e_{31} & e_{31} & e_{33} & \varepsilon_{33}\end{bmatrix}^{-1}, \quad \begin{bmatrix} s_{44} & g_{15}\\ -g_{15} & \beta_{11}\end{bmatrix} = \begin{bmatrix} c_{44} & -e_{15}\\ e_{15} & \varepsilon_{11}\end{bmatrix}^{-1} \tag{B2}$$

We recall that, essentially without loss of generality, no body loads are considered and the plate is assumed to be clamped and grounded along its lateral boundary $\partial\Omega\times(-t/2,t/2)$. If this were not the case, straightforward modifications of $\mathscr{H}$ would be needed, but the present derivation of the plate model would remain essentially unchanged.

With a view toward deriving the plate model, a partially mixed formulation is obtained from (B1), by enforcing *a priori* the stationarity conditions of $\mathscr{H}$ with respect to $\mathbf{T}$ and $\boldsymbol{d}$. After simple computations, we obtain

$$\begin{aligned}\mathscr{R} = \frac{1}{2}\int_A \Bigg[&2c_{66}||\boldsymbol{\nabla}^S\boldsymbol{S}||^2 + \hat{c}_{12}(\operatorname{div}\boldsymbol{S})^2 - \frac{\varepsilon_{33}}{c_{33}\bar{\varepsilon}_{33}}\sigma^2 + \frac{1}{\bar{\varepsilon}_{33}}d^2 + 2\frac{\hat{\bar{e}}_{33}}{\bar{\varepsilon}_{33}}\sigma(\operatorname{div}\boldsymbol{S}) - 2\frac{\bar{e}_{31}}{\bar{\varepsilon}_{33}}d(\operatorname{div}\boldsymbol{S})\\ &-2\frac{e_{33}}{c_{33}\bar{\varepsilon}_{33}}\sigma d - \frac{1}{c_{44}}||\boldsymbol{\tau}||^2 - \bar{\varepsilon}_{11}||\boldsymbol{\nabla}\Phi||^2 + 2\frac{e_{15}}{c_{44}}\boldsymbol{\tau}\cdot\boldsymbol{\nabla}\Phi\Bigg]\,\mathrm{d}v\end{aligned}$$

$$+\int_A [\boldsymbol{\tau}\cdot(\boldsymbol{S}'+\boldsymbol{\nabla}S)+\sigma S'+d\Phi']\,\mathrm{d}v$$

$$-\int_\Omega [\boldsymbol{P}^{\pm}\cdot\boldsymbol{S}(\cdot,\pm t/2)+P^{\pm}S(\cdot,\pm t/2)-\Upsilon^{\pm}\Phi(\cdot,\pm t/2)]\,\mathrm{d}a-\int_{\partial\Omega\times(-t/2,t/2)}(\boldsymbol{\tau}\cdot\boldsymbol{n})S\,\mathrm{d}a \quad \text{(B3)}$$

defined on the manifold: $\boldsymbol{S}=0$ and $\Phi=0$ on $\partial\mathscr{A}$. Here $\hat{\varepsilon}_{33}=(c_{13}\varepsilon_{33}+e_{31}e_{33})/c_{33}$. The functional $\mathscr{R}$ is the extension to piezoelectric bodies of a functional introduced by Reissner [18].

Needless to say that the variational formulations (B1) and (B3) are *exact* consequences of the Voigt theory of piezoelectricity. In order to derive models of piezoelectric plates, simplifying hypotheses concerning the structure of the involved fields have to be introduced.

The hypotheses underlying the model proposed in Reference [10] are:

(i) the transversal normal strain S' vanishes;
(ii) the transversal shear strain $\boldsymbol{\nabla}S+\boldsymbol{S}'$ is constant in the thickness;
(iii) the transversal electric field $-\Phi'$ is constant in the thickness.

The approximations introduced by these hypotheses are mitigated [19] by complementing them with the following 'dual' hypotheses:

(i′) the transversal normal stress σ vanishes;
(ii′) the transversal shear stress $\boldsymbol{\tau}$ is constant in the thickness;
(iii′) the transversal electric displacement field d is constant in the thickness.

The hypotheses (i), (ii) and (i′) are the classical hypotheses of the Reissner–Mindlin theory of elastic plates. The hypothesis (iii) was introduced first in Reference [2], then enforced, among others, in References [3] and [8]. The hypothesis (ii′) was adopted in Reference [2]. It is emphasized that none of the previous hypothesis is a rigorous assumption, even if the plate thickness aspect ratio approaches zero [20]. As a matter of fact, this 'drawback' is shared by the celebrated Reissner–Mindlin theory of elastic plates, since it is well known that elastic plates do not fulfil any of the hypotheses (i), (ii) and (i′), even if the plate thickness aspect ratio approaches zero. Of course, it is the very essence of a modelization to retain only some features of a complex problem and to neglect the remaining ones. As it is shown in appendix C, the piezoelectric plate model proposed in Reference [10] is able to grasp the main features of the problem, in most of practical situations.

As a consequence of the hypotheses (i), (ii) and (iii), the displacement field and the electric potential field can be represented by means of the unknown functions $\boldsymbol{U}$, W, $\boldsymbol{\Theta}$, Π and X, defined over the two-dimensional region Ω, according to Equation (2). Analogously, as a consequence of the hypotheses (i′), (ii′) and (iii′), the transversal normal- and shear-stress fields and the transversal electric-displacement field can be represented by means of the unknown functions $\boldsymbol{V}$ and D, defined over the two-dimensional region Ω, according to the equations

$$\begin{aligned}\sigma(\boldsymbol{Y},\zeta)&=0\\ \boldsymbol{\tau}(\boldsymbol{Y},\zeta)&=\boldsymbol{V}(\boldsymbol{Y})\\ d(\boldsymbol{Y},\zeta)&=D(\boldsymbol{Y})\end{aligned} \quad \text{(B4)}$$

By substituting the representation formulas (2) and (B4) into Equation (B3) and performing the integration with respect to the thickness variable ζ, the functional $\mathscr{R}$ is transformed into

$$\mathscr{P} = \mathscr{P}_{\mathrm{m}} + \mathscr{P}_{\mathrm{b}} \tag{B5}$$

where

$$\mathscr{P}_{\mathrm{m}} = \frac{t}{2}\int_{\Omega}\left[2c_{66}||\boldsymbol{\nabla}^{S}\boldsymbol{U}||^{2} + \hat{c}_{12}(\operatorname{div}\boldsymbol{U})^{2} + \frac{1}{\bar{\varepsilon}_{33}}D^{2} - 2\frac{\bar{e}_{31}}{\bar{\varepsilon}_{33}}D(\operatorname{div}\boldsymbol{U})\right]\mathrm{d}a$$
$$-\frac{t^{3}}{24}\int_{\Omega}\bar{\varepsilon}_{11}||\boldsymbol{\nabla}X||^{2}\,\mathrm{d}a + t\int_{\Omega}DX\,\mathrm{d}a - \int_{\Omega}(\boldsymbol{R}^{*}\cdot\boldsymbol{U} - \Upsilon^{*}X)\,\mathrm{d}a \tag{B6}$$

and

$$\mathscr{P}_{\mathrm{b}} = \frac{t^{3}}{24}\int_{\Omega}[2c_{66}||\boldsymbol{\nabla}^{S}\boldsymbol{\Theta}||^{2} + \hat{c}_{12}(\operatorname{div}\boldsymbol{\Theta})^{2}]\,\mathrm{d}a + \frac{t}{2}\int_{\Omega}\left[-\frac{1}{c_{44}}||\boldsymbol{V}||^{2} - \bar{\varepsilon}_{11}||\boldsymbol{\nabla}\Pi||^{2} + 2\frac{e_{15}}{c_{44}}\boldsymbol{V}\cdot\boldsymbol{\nabla}\Pi\right]\mathrm{d}a$$
$$+t\int_{\Omega}\boldsymbol{V}\cdot(\boldsymbol{\Theta}+\boldsymbol{\nabla}W)\,\mathrm{d}a - t\int_{\partial\Omega}(\boldsymbol{V}\cdot\boldsymbol{n})W\,\mathrm{d}l - \int_{\Omega}(\boldsymbol{M}^{*}\cdot\boldsymbol{\Theta} + R^{*}W - \Psi^{*}\Pi)\,\mathrm{d}a \tag{B7}$$

The functional $\mathscr{P}$ is defined on the manifold: $\boldsymbol{U}=0$, $X=0$, $\boldsymbol{\Theta}=0$ and $\Pi=0$ on $\partial\Omega$. It completely characterizes the piezoelectric plate model proposed in Reference [10].

In order to derive the field equations (3) and (4) presented in Section 2, a total-potential-energy functional is carried out. It is obtained by enforcing *a priori* the stationarity conditions of $\mathscr{P}$ with respect to D and $\boldsymbol{V}$. After simple calculations, we get the functional

$$\mathscr{E} = \mathscr{E}_{\mathrm{m}} + \mathscr{E}_{\mathrm{b}} \tag{B8}$$

where

$$\mathscr{E}_{\mathrm{m}} = \frac{t}{2}\int_{\Omega}[2c_{66}||\boldsymbol{\nabla}^{S}\boldsymbol{U}||^{2} + \bar{c}_{12}(\operatorname{div}\boldsymbol{U})^{2} - \bar{\varepsilon}_{33}X^{2} + 2\bar{e}_{31}X(\operatorname{div}\boldsymbol{U})]\,\mathrm{d}a$$
$$-\frac{t^{3}}{24}\int_{\Omega}\bar{\varepsilon}_{11}||\boldsymbol{\nabla}X||^{2}\,\mathrm{d}a - \int_{\Omega}(\boldsymbol{R}^{*}\cdot\boldsymbol{U} - \Upsilon^{*}X)\,\mathrm{d}a \tag{B9}$$

and

$$\mathscr{E}_{\mathrm{b}} = \frac{t^{3}}{24}\int_{\Omega}[2c_{66}||\boldsymbol{\nabla}^{S}\boldsymbol{\Theta}||^{2} + \hat{c}_{12}(\operatorname{div}\boldsymbol{\Theta})^{2}]\,\mathrm{d}a + \frac{t}{2}\int_{\Omega}[c_{44}||\boldsymbol{\Theta}+\boldsymbol{\nabla}W||^{2} + 2e_{15}(\boldsymbol{\Theta}+\boldsymbol{\nabla}W)\cdot\boldsymbol{\nabla}\Pi$$
$$-\varepsilon_{11}||\boldsymbol{\nabla}\Pi||^{2}]\,\mathrm{d}a - \int_{\Omega}(\boldsymbol{M}^{*}\cdot\boldsymbol{\Theta} + R^{*}W - \Psi^{*}\Pi)\,\mathrm{d}a \tag{B10}$$

The functional $\mathscr{E}$ is defined on the manifold: $\boldsymbol{U}=0$, $X=0$, $W=0$, $\boldsymbol{\Theta}=0$ and $\Pi=0$ on $\partial\Omega$. It is an easy task to verify that the field equations (3) of the membranal problem are obtained as stationary conditions of $\mathscr{E}$ with respect to $\boldsymbol{U}$ and X, and the field equations (4) of the bending problem are

obtained as stationary conditions of $\mathscr{E}$ with respect to $\boldsymbol{\Theta}$, W and Π. Of course, this variational formulation supplies also the compatible boundary operators [21], which are not reported here for the sake of brevity.

APPENDIX C: A CRITICAL EVALUATION OF THE PIEZOELECTRIC PLATE MODEL

In this section, in order to emphasize the scope of the model proposed in Reference [10] and adopted in this paper, we refer to the problems introduced in Section 4 and present a thorough *analytical* comparison between the results supplied by the present model, reported in Section 4, and the ones supplied by the Voigt theory of piezoelectricity, reported in what follows. To the authors' knowledge, such an analytical comparison was not performed for other existing models of piezoelectric plates.

C.1 Membranal problems

The loading conditions are the ones considered in Section 4.1. Under those loading conditions, explicit solutions, computed in the framework of the Voigt theory of piezoelectricity, are available in the literature [20]. Those solutions were expanded in Reference [20] as power series of the slenderness parameter δ, and the leading-order terms of the expansions are reported here:

- Load a:

$$\boldsymbol{u} = \frac{r_0}{2\pi^2(1+\xi^2)} \begin{bmatrix} \cos(\pi y_1)\sin(\pi y_2) \\ \sin(\pi y_1)\cos(\pi y_2) \end{bmatrix} + o(1)$$

$$s = \frac{\hat{\varepsilon}_{33} r_0}{\pi(1+\xi^2)\bar{\varepsilon}_{33}} z \sin(\pi y_1)\sin(\pi y_2) + o(1)$$

$$\chi = -\frac{\xi r_0}{\pi(1+\xi^2)} \sin(\pi y_1)\sin(\pi y_2) + o(1)$$

- Load b:

$$\boldsymbol{u} = \frac{r_0}{\pi^2(1-\nu)} \begin{bmatrix} \cos(\pi y_1)\sin(\pi y_2) \\ -\sin(\pi y_1)\cos(\pi y_2) \end{bmatrix} + o(1)$$

$$s = 0$$

$$\chi = 0$$

- Load c:

$$\boldsymbol{u} = \frac{\xi \upsilon_0}{2\pi(1+\xi^2)} \begin{bmatrix} \cos(\pi y_1)\sin(\pi y_2) \\ \sin(\pi y_1)\cos(\pi y_2) \end{bmatrix} + o(1)$$

$$s = -\frac{\upsilon_0(e_{33}c_{11} - c_{13}e_{31})}{(1+\xi^2)c_{33}\sqrt{\bar{\varepsilon}_{33}\bar{c}_{11}}} z \sin(\pi y_1)\sin(\pi y_2) + o(1)$$

$$\chi = \frac{\upsilon_0}{1+\xi^2} \sin(\pi y_1)\sin(\pi y_2) + o(1)$$

where $s = S/t$, $z = \zeta/t$ and $o(\cdot)$ is the Landau symbol.

It is emphasized that in all load cases the leading-order terms of the Voigt solutions for $\boldsymbol{u}$ and χ are *exactly* coincident with the leading-order terms of the solutions supplied by the model proposed in Reference [10]. Hence, in particular, this model accounts for the correct value of the membrane mechanical stiffness, electric capacity and piezoelectric coupling. The model proposed in Reference [10] is unable to give s, due to the hypothesis (i) introduced in Appendix B. This drawback, which is shared by most of existing models of piezoelectric plates and even by the celebrated Reissner–Mindlin theory of elastic plates, is almost always negligible in practical applications. In situations where the computation of s could be useful, the model proposed in Reference [8] would be indicated.

C.2. Bending problems

The loading conditions are the ones considered in Section 4.2. As in the previous case, explicit solutions, computed in the framework of the Voigt theory of piezoelectricity, are available in the literature [20]. The leading-order terms of their expansions as power series of the slenderness parameter ε are reported here:

- Load a:

$$\boldsymbol{\theta} = -\frac{r_0}{4\pi^3}\begin{bmatrix}\cos(\pi y_1)\sin(\pi y_2)\\ \sin(\pi y_1)\cos(\pi y_2)\end{bmatrix} + o(1)$$

$$w = \frac{r_0}{4\pi^4}\sin(\pi y_1)\sin(\pi y_2) + o(1)$$

$$\beta = \frac{\kappa r_0}{2\pi^2}\varepsilon^2\left[1 + \frac{\bar{\varepsilon}_{11}c_{44}\bar{e}_{31}}{\bar{\varepsilon}_{33}\hat{c}_{11}e_{15}}\left(6z^2 - \frac{1}{2}\right)\right]\sin(\pi y_1)\sin(\pi y_2) + o(\varepsilon^2)$$

- Load b:

$$\boldsymbol{\theta} = \frac{m_0}{2\pi^2}\begin{bmatrix}\cos(\pi y_1)\sin(\pi y_2)\\ \sin(\pi y_1)\cos(\pi y_2)\end{bmatrix} + o(1)$$

$$w = -\frac{m_0}{2\pi^3}\sin(\pi y_1)\sin(\pi y_2) + o(1)$$

$$\beta = -\frac{\bar{e}_{31}\sqrt{\bar{\varepsilon}_{11}c_{44}}}{\pi\hat{c}_{11}\bar{\varepsilon}_{33}}m_0\varepsilon^2\left(6z^2 - \frac{1}{2}\right)\sin(\pi y_1)\sin(\pi y_2) + o(\varepsilon^2)$$

- Load c:

$$\boldsymbol{\theta} = m_0\varepsilon^2\begin{bmatrix}\cos(\pi y_1)\sin(\pi y_2)\\ -\sin(\pi y_1)\cos(\pi y_2)\end{bmatrix} + o(\varepsilon^2)$$

$$w = 0$$

$$\beta = 0$$

- Load d:

$$\boldsymbol{\theta} = \frac{\psi_0}{2\pi} \frac{\bar{e}_{31}\sqrt{c_{44}\bar{\varepsilon}_{11}}}{\hat{c}_{11}\bar{\varepsilon}_{33}} \begin{bmatrix} \cos(\pi y_1)\sin(\pi y_2) \\ -\sin(\pi y_1)\cos(\pi y_2) \end{bmatrix} + o(1)$$

$$w = -\frac{\psi_0}{2\pi^2} \left[\kappa + \frac{\bar{e}_{31}\sqrt{c_{44}\bar{\varepsilon}_{11}}}{\hat{c}_{11}\bar{\varepsilon}_{33}} \right] \sin(\pi y_1)\sin(\pi y_2) + o(1)$$

$$\beta = \frac{\psi_0}{2\pi^2} \sin(\pi y_1)\sin(\pi y_2) + o(1)$$

We emphasize that in the situations corresponding to load cases a, b and c the model proposed in Reference [10] supplies very satisfactory results. In particular, it accounts for the correct bending stiffness of the piezoelectric plate, and this is a very valuable feature in practical applications. Indeed, the leading-order terms of the solutions for $\boldsymbol{\theta}$ and w that it supplies are *exactly* coincident with the leading-order terms of the Voigt solution. Moreover, since $\int_{-1/2}^{1/2}(6z^2 - 1/2)\,\mathrm{d}z = 0$, we point out that the model proposed in Reference [10] supplies the *exact* mean value of the electric potential: this is of course the best result obtainable under the assumption (iii) introduced in Appendix B and is sufficient for most of practical applications. A less satisfactory result is obtained in the situations corresponding to load case d, since only the electric potential is exactly estimated. More satisfactory results in these situations could be obtained by using the higher-order model proposed in Reference [9], or, alternatively, by using the model proposed in Reference [10] in the framework of a layer-wise modellization of the plate, regarded as a bilayer structure [22]. As a matter of fact, load case d involves electric-charge distributions with the same sign on the two surfaces of the plate: this is completely unrealistic, since in applications a piezoelectric plate used as a sensor or an actuator behaves as a capacitor, and hence the electric-charge distributions have opposite signs on the two surfaces. We can conclude that the model proposed in Reference [10] joins the simplicity and easiness of a first-order model with the ability to supply results which are very valuable in practical applications.

REFERENCES

1. Ikeda T. *Fundamentals of Piezoelectricity*. Oxford University Press: Oxford, 1990.
2. Mindlin RD. High frequency vibrations of piezoelectric crystal plates. *International Journal of Solids and Structures* 1972; **8**:895–906.
3. Dökmeci MC. Theory of vibrations of coated, thermopiezoelectric laminae. *Journal of Mathematical Physics* 1978; **19**:109–126.
4. Maugin GA, Attou D. An asymptotic theory of thin piezoelectric plates. *Quarterly Journal of Mechanics and Applied Mathematics* 1990; **43**:347–362.
5. Tiersten HF. Equations for the control of the flexural vibrations of composite plates by partially electroded piezoelectric actuators. In *Active Materials and Smart Structures*, Anderson GL, Lagoudas DC (eds). SPIE Proceedings Series, vol 2437, 1994; 326–342.
6. Tzou HA. *Piezoelectric Shells* Kluwer Academic Publishers: Dordrecht, 1993.
7. Yang JS. Equations for elastic plates with partially electroded piezoelectric actuators in flexure with shear deformation and rotatory inertia. *Journal of Intelligent Material Systems and Structures* 1997; **8**:444–451.
8. Nicotra V, Podio-Guidugli P. Piezoelectric plates with changing thickness. *Journal of Structural Control* 1998; **5**: 73–86.
9. Yang JS. Equations for thick elastic plates with partially electroded piezoelectric actuators and higher order electric fields. *Smart Materials and Structures* 1999; **8**:73–82.
10. Bisegna P. A theory of piezoelectric laminates. *Rendiconti di Matematica & Applicazioni dell' Accademia dei Lincei* (s. 9) 1997; **8**:137–165.
11. Bisegna P, Maceri F. A consistent theory of thin piezoelectric plates. *Journal of Intelligent Materials Systems and Structures* 1996; **7**:372–389.

12. Auricchio F, Lovadina C. Analysis of kinematically linked interpolation methods for Reissner–Mindlin plate problems. *Computer Methods in Applied Mechanics and Engineering*, to appear.
13. Auricchio F, Taylor RL. A shear deformable plate element with an exact thin limit. *Computer Methods in Applied Mechanics and Engineering* 1994; **118**:393–412.
14. Brezzi F, Fortin M. *Mixed and Hybrid Finite Element Method*. Springer: Berlin, 1991.
15. Ciarlet PG. *The Finite Element Method for Elliptic Problems*. North Holland: Amsterdam, 1978.
16. Zienkiewicz OC, Taylor RL. *The Finite Element Methods*. McGraw-Hill: New York, NY, 1989.
17. Chenais D, Paumier JC. On the locking phenomenon for a class of elliptic problems. *Numerical Mathematics* 1994; **67**:427–440.
18. Reissner E. On a certain mixed variational theorem and a proposed application. *International Journal for Numerical Methods in Engineering* 1984; **20**:1366–1368.
19. Teresi L, Tiero A. On variational approaches to plate models. *Meccanica* 1997; **32**:143–156.
20. Bisegna P, Maceri F. An exact three-dimensional solution for simply supported rectangular piezoelectric plates. *Journal of Applied Mechanics* 1996; **63**:628–638.
21. Lions JL, Magenes E. *Problèmes aux limites non homogènes et applications*. Dunod: Paris, 1968.
22. Bisegna P, Caruso G, Maceri F. Refined models for vibration analysis and control of thick piezoelectric laminates. In *Optimization and Control in Civil and Structural Engineering*, Topping BHV, Kumar B (eds). Civil-Comp Press: Edinburgh, 1999.
23. Bernadou M, Haenel D. Some remarks about piezoelectric shells. In *Advances in Finite Element Techniques*, Papadrakakis M, Topping BHV (eds). Saxe-Coburg Publications: Edinburgh, 1994; 1–7.

